Population burdens of air pollution around the world: Distributions, inequalities, and links to per capita GDP

Preliminary draft

The latest version of this paper is available at this link.

Angelo Santos, Oscar Morales, Jere R. Behrman, Emily Hannum, Fan Wang*

November 20, 2024

Abstract

We analyze the global population-weighted distribution of air pollution by aerosols and its relationship to GDP per capita. We first decompose the global distribution and consider both variations across and within regions and countries. Second, we map national and subnational distributions of air pollution by aerosols to national and subnational distributions of GDP per capita. We find considerable global exposure inequalities. Comparing continents at the extremes, the average individual in Asia is 3.32 times more exposed to air pollution by aerosols than the average individual in Oceania. In Africa and Asia, populations at the 80^{th} percentile of the air pollution by aerosol distribution are 141% and 109% more exposed than population at the 20^{th} percentile, and those at the 90^{th} percentile are 227% and 185% more exposed those at the 10^{th} percentile. Globally, we find that a doubling of GDP per capita is associated with a 11.8 percentage points reduction in the percentage deviation between a subnational unit's population-weighted air pollution by aerosol level and the global population-weighted mean. Within each continent, exploiting variabilities in subnational data after controlling for aggregate regional variabilities, we find positive associations between air pollution by aerosols and GDP per capita in Africa and Europe, but negative associations in the Americas, Asia, and Oceania.

*Angelo Santos: Department of Economics, University of Houston, Houston, Texas, USA; Oscar Morales: Department of Economics, University of Houston, Houston, Texas, USA; Jere R. Behrman: Departments of Economics and Sociology and Population Studies Center, University of Pennsylvania, Philadelphia, PA 19104, USA; Emily Hannum: Department of Sociology and Population Studies Center, University of Pennsylvania, PA, USA; Fan Wang: Department of Economics, University of Houston, Houston, Texas, USA. This paper is part of the project "Climate Risk, Pollution, and Childhood Inequalities in Low- and Middle-income Countries," which is supported by National Science Foundation Grant 2230615 (PI: Hannum)

1 Introduction

Air-pollution exposure has been increasing over time and growing evidence has pointed to this exposure as a high-risk factor for global health (Gakidou et al. 2017). Fine-particulate-matter exposure, especially to $PM_{2.5}$, has been implicated as the cause of millions of deaths around the world, and negatively correlated with outcomes such as health, children's cognitive development, and productivity (Fisher et al. 2021; Fu, Viard, and Zhang 2021; Odo et al. 2023). Additionally, more than half of the global population is exposed to shallow quality air (PM2.5 concentrations of more than 35 $\mu g/m^3$) and this exposure has been increasing over time (Pirlea and Huang 2019; Shaddick et al. 2020). As pollution exposure worsens across the world, it is ever more important to examine the distributional effects this has on global populations to better understand what parts of the world are most or least affected in order to better design potential policy interventions.

A large literature already documents changing patterns of global climatic and pollution exposure but generally focuses on variations in climatic measures across locations and time, without tying the data to the geographical distribution of the population experiencing these changes (Mehta et al. 2016; Tian et al. 2023). In social science, there is also a rapidly growing empirical literature that uses available micro-data from parts of the world to estimate the effects of pollution exposures on labor market productivity, health, as well as educational outcomes (Brabhukumr et al. 2020; Gakidou et al. 2017; Odo et al. 2023). These papers, however, do not provide global analyses of the overall pollution burdens facing population from across the world.

This paper contributes to burgeoning literature that combines global population distribution and global air pollutant measurements to study global heterogeneities in population-weighted air pollution burden (Shaddick et al. 2018; Van Donkelaar et al. 2021). Prior papers in this literature have generally focused on comparing regional and national mean measures. Our paper is the first to analyze inequalities in air pollution distributions across and within regions and countries of the world. We accomplish this by decomposing the global population-weighted air pollution distribution into across and within region and country components.

Additionally, we provide the first global analysis that maps global national and subnational variations in air pollution to economic development as captured by GDP per capita. We provide results on the direction and magnitude of the GDP per capita and air pollution associ-

ation globally and for each continent, and use continental and regional fixed effects to explain whether aggregate associations are due to across region or within region variabilities.

Our analysis is based on gridded high-resolution global data on pollution and population and subnational GDP per capita data from around 2010, the year around which globally reliable measures of air pollution, population and GDP are available. For air pollution, we use data on air pollution by aerosols, as captured by satellite-based Aerosol Optical Depth (AOD) measurements (Xiong et al. 2020). We combine the air pollution by aerosol data with gridded granular national population census and population register data (CIESIN Columbia University 2018). We compute in particular the relative burden of air pollution by aerosol facing population in a particular gridded cell versus the global population-weighted mean exposure, and we construct country-specific population distributions of air pollution burden based on the geographical dispersion of population and air pollution within each country. Finally, we combine the population-weighted air pollution data, aggregated to subnational levels, with subnational GDP per capita data (Gennaioli et al. 2013; Kummu, Taka, and Guillaume 2018).

We find considerable global inequalities in population-weighted air pollution by aerosol exposures. Population in Asia, the continent with the highest level of air pollution by aerosols, face a mean exposure level that is 3.3 times larger than those faced by population in Oceania, which has the lowest mean exposure among continents. Looking across regions within continents, we find that in Eastern Asia, the subcontinental region with the highest level of air pollution by aerosols, the population faces a mean exposure level that is 6.0 times larger than that faced by the population in Australia and New Zealand, which have the lowest mean exposure among subcontinental regions,

In terms of inequalities, across continents, population at the 80^{th} percentile of the continental air pollution by aerosol distribution have between 28% (Europe) to 141% (Africa) greater air pollution by aerosol exposures than population at the 20^{th} percentile. Across subcontinental regions, population at the 80^{th} percentile of the regional air pollution by aerosol distribution have between 2% to 208% greater air pollution by aerosol exposures than population at the 20^{th} percentile. Within countries, population at the 80^{th} percentile of country-specific air pollution by aerosol distributions have between 0% to 359% greater air pollution by aerosol exposures than population at the 20^{th} percentile.

For the global GDP per capita and air pollution by aerosol analysis, overall, we find a strong negative global correlation. This indicates that globally, national and subnational economic

units with higher GDP per capita tend to have lower air pollution by aerosols. Specifically, using subnational population-weighted data, we find that a doubling of GDP per capita is associated with a 11.8 percentage points reduction in the percentage deviation between a subnational unit's population-weighted air pollution by aerosol level and the global population-weighted mean. This global association is largely explained by correlation between continental-level mean GDP per capita and air pollution by aerosol.

Furthermore, we analyze the GDP and air pollution relationship within each continent. Exploiting variabilities in subnational data after controlling for aggregate regional variabilities, we find a positive association between air pollution by aerosols and GDP per capita in Africa and Europe, but negative association in the Americas, Asia, and Oceania.

2 Data and Methods

2.1 Data and aggregation

Air pollution by aerosols as measured by AOD Aerosols are ensembles of suspended particles present in the Earth's atmosphere. Atmospheric pollution by aerosols is important to human health and well-being because higher amounts of aerosol particles degrade visibility and can also damage health, especially when there is a higher concentration of $PM_{2.5}$ particles that are smaller then 2.5 micrometers (Jacobson 2002). Aerosol Optical Depth (AOD) is a satellite-based measure that captures the composition, size and concentration of aerosols by measuring the magnitude of atmospheric light reflection and absorption across the globe (Lenoble, Remer, and Tanre 2013). Scaled between 0 to 1, an AOD value that is less than 0.1 indicates crystal clear sky and clear satellite to earth surface visibility. In contrast, an AOD value close to 1 indicates very hazy conditions (NASA Earth Observatory 2024).

We use AOD measurements based on images collected by the TERRA satellite with its MODIS instruments (Xiong et al. 2020), and we access the data via the NASA EarthData data collection, using the OpenDAP protocol (Cornillon, Gallagher, and Sgouros 2003). On each day in a particular year, tracking along TERRA's orbital path across the globe, we download AOD data at a spatial resolution of 3km $\times$ 3km and at all available 5 minute temporal resolution units. For each day, this process generates a vector of latitude-, longitude-, and time-specific AOD measurements.

Within each $1^\circ \times 1^\circ$ longitude–latitude grid (cell), we compute average daily AOD values

based on the subset of the daily AOD measurement vector that fall within the geographical boundaries of each cell on that day. Repeating this across days during a year, we generate for each cell, a vector of average daily AOD measurements. During each year, the length of these cell-specific daily average AOD vectors is equal to the number of days in which valid AOD measurements are available for a particular cell. On some days, there might be no cell-specific AOD measurements due to high cloud fraction and invalid reflectance assumptions (Wang et al. 2021) or due to limited overlaps between the cells and the daily orbital path (Xiong et al. 2020).

Using the cell-specific vectors of average daily AOD measurements from a year, we compute annual average AOD exposures for each cell, first averaging over the days in which cell-specific measurements are available, and then separately averaging over all days after complementing the observed averages with interpolated and extrapolated estimates on days without cell-specific measurements. Due to the concentration of missing AOD data in regions with the least population, our population-weighted AOD distributional results based on the raw data and interpolated and extrapolated data are very similar. Our global inequality results presented in the text are based on annual averages of the raw data.[1]

Global gridded population data In conjunction with the cell-specific AOD data, we generate cell-specific global population estimates based on the Gridded Population of the World Version 4 (GPWv4) dataset from the Center for International Earth Science Information Network (CIESIN Columbia University 2018). The GPWv4 data contains population statistics from 241 global economies. Data is sourced in most cases from national and local statistical agencies, and when that is not available, sourced from the United Nations.

The gridded GPWv4 data provides total population estimates at 30 arc-second grids ($\sim$ 1km at the equator), and is globally disaggregated from official population data at the smallest administrative level available. As an illustration, the dataset contains disaggregated population data from 316,461 Brazilian sectors, 43,878 Chinese townships, 5,967 Indian sub-districts, 774 Nigerian local government areas, and 10,535,212 US census blocks. To allow for the calculation population-weighted AOD data, we aggregate the GPWv4 population estimates up to $1^\circ \times 1^\circ$ longitude–latitude grid, which matches up with the resolution of our cell-specific annual average AOD exposures data.

1. See Appendix Figure E.1 for a visualization of the number of days in 2010 with AOD measurements across global cells.

Due to variabilities in census survey and population register data availability, GPWv4 population data are sourced between the years 2001 and 2015, with the center of the calendar year distribution at around 2010. Specifically, data from 27% of the economies are based on 2010 census and population register data, 62% and 83% of the economies' data come from within one and three years of 2010, and about 8% of the economies have data sourced from outside of four years of 2010. To appropriately match up the time-frame of the population and AOD data, we use cell-specific annual average AOD exposure data in 2010.

Subnational GDP data We complement global measurements of air pollution by aerosols and population with data on the relative levels of economic development as captured by GDP per capita. Specifically, we use national and subnational from the Gridded global datasets for Gross Domestic Product (Kummu, Taka, and Guillaume 2018), which is based on subnational GDP per capita data from Gennaioli et al. (2013). The GDP per capita values are adjusted for purchasing price parity and based on 2005 international dollars.

Gennaioli et al. (2013) collected subnational GDP data from 1569 subnational first-level or equivalent administrative units from the largest 110 economies up to 2010. These economies accounted for 97% of global GDP in 2010. Kummu, Taka, and Guillaume (2018) augmented the dataset with national GDP data from economies without subnational data, filling in missing subnational GDP values by interpolating based on geographically and temporally neighboring data-points around missing values, and extended the dataset time-frame to 2015 by extrapolating based on trends up to 2010.

Considering jointly the temporal availability of AOD, pollution, and GDP data, we use the 2010 subnational and national GDP per capita estimates from Kummu, Taka, and Guillaume (2018).

2.2 Population weighted distributional statistics for AOD

Population-weighted AOD distributions To analyze population-weighted air pollution by aerosol distributions, we define a discrete distribution of 2010 annual average AOD values over the set of all populated cells, where the cell-specific population mass is determined by GPWv4-based population estimates from around 2010. Specifically, let s_c be the share of global population in cell c, a_c be the average annual AOD at cell c, and C be the set of all gridded cells where $s_c > 0$. The global population-weighted annual average AOD distribution function,

which provides the share of global population experiencing lower than a^* levels of annual average AOD, is equal to:

$$F(a^*) = P(a < a^*) = \sum_{c \in C} s_c \cdot \mathbf{1}\{a_c < a^*\} \ . \tag{1}$$

To compare aerosol distributions conditional on regional groupings based on supranational, national, and subnational boundaries, we define $C_r \subseteq C$ as the set of populated cells that intersect with the boundary enclosures of supranational, national, or subnational location r. For boundary data, we use national boundary data available in the GPWv4 population dataset (CIESIN Columbia University 2018), and the subnational boundary data embedded in the subnational GDP data from (Kummu, Taka, and Guillaume 2018). The share of population in cell c conditional on location grouping r is $s_{c,r} = \frac{s_c}{(\sum_{\hat{c} \in C_r} s_{\hat{c}})}$, and the locational AOD distribution function is:

$$F_r(a^*) = P_r(a < a^*) = \sum_{c \in C_r} s_{c,r} \cdot \mathbf{1}\{a_c < a^*\} \ . \tag{2}$$

Given the locational distribution function, we compute key distributional statistics for each location r. The mean and variance of the location r-specific distributions are

$$\begin{aligned} \mu_r &= \sum_{c \in C_r} s_{c,r} \cdot a_c \\ \text{and } \sigma_r^2 &= \sum_{c \in C_r} s_{c,r} \cdot (a_c - \mu_r)^2 \ . \end{aligned} \tag{3}$$

The global weighted mean is $\mu_{\text{global}} = \sum_{c \in C} s_c \cdot a_c$. In our empirical analysis, we compute global, continental, regional, national, and subnational population weighted annual mean AOD exposures.

Given the discrete mass distribution over cells, the location distribution function $F_r(a^*)$ is not invertible. Hence, we define the τ^{th} percentile of the locational distribution as the minimum a^* value where the share of population in location r with less than a^* level of annual average AOD is greater or equal to $\frac{\tau}{100}$, specifically:

$$\text{percentile}_r(\tau) = \min \left\{ a^* : F_r(a^*) \geqslant \frac{\tau}{100} \right\} \ . \tag{4}$$

Discussions in our empirical analysis focus on location-specific 20^{th} and 80^{th} as well as 10^{th} and

90^{th} percentiles, and use relative percentile ratios as an additional measures for within location distributional variabilities.

Relative exposure and excess burden To measure relative exposures, we compute what we call excess aerosol burden, $e_{c,\widehat{r}}$, which is the percentage deviation between cell-specific AOD value a_c and location-specific AOD value average $\mu_{\widehat{r}}$:

$$e_{c,\widehat{r}} = \frac{a_c - \mu_{\widehat{r}}}{\mu_{\widehat{r}}} = \frac{a_c}{\mu_{\widehat{r}}} - 1 \ . \tag{5}$$

When $\widehat{r}$ includes all global cells, we have $e_{c,\text{global}}$, the global excess aerosol burden. We also divide weighted mean from location r against that of another location $\widehat{r}$:

$$e_{r,\widehat{r}} = \frac{\mu_r - \mu_{\widehat{r}}}{\mu_{\widehat{r}}} = \frac{\mu_r}{\mu_{\widehat{r}}} - 1 \ . \tag{6}$$

When r is a country and $\widehat{r}$ includes all global cells, $e_{\text{country,global}}$ is the country-specific excess aerosol burdens relative to the global mean. A global excess aerosol value of 0 indicates that a location has the same AOD measure as the global mean, and a value of 0.5 or -0.5 indicates that a location's AOD measure is 50 percent greater or smaller than the global mean.

As an additional interpretation of the ratio of the weighted means of a subset over a superset, $e_{r,\text{global}}$ can also be expressed as:

$$e_{r,\text{global}} = \frac{\overbrace{\left(\frac{\left(\sum_{c \in C_r} s_c\right) \cdot \mu_r}{\mu_{\text{global}}}\right)}^{\text{Location r pop-weighted pollution share}}}{\underbrace{\left(\sum_{c \in C_r} s_c\right)}_{\text{Location r population share}}} - 1 = \frac{\mu_r}{\mu_{\text{global}}} - 1 \ . \tag{7}$$

A value of 0.5 or -0.5 for $e_{r,\text{global}}$ indicates that location r's share of global population-weighted air pollution is 50 percent greater or smaller than location r's share of global population.

AOD and $PM_{2.5}$ As a satellite-based measure of air pollution by aerosols, AOD measurements increase with greater concentrations of atmospheric particles, including $PM_{2.5}$ particles. While our analysis is focused on the distribution of air pollution by aerosols as measured by AOD, to help provide additional interpretation of our AOD results, in our presentation and discussion of results, we provide results both in AOD as well as in estimated AOD-

transformed $PM_{2.5}$ scales.

While AOD captures directly visibility experiences, the best-fitting model that maps between atmospheric aerosol measurements and on-the-ground ambient particulate matter exposure experienced by people is parameterized by heterogeneous topological and meteorological circumstances (Chu et al. 2016; Holben et al. 1998; Van Donkelaar et al. 2016; Yang et al. 2019). Overall, atmospheric-based AOD measures have been found to substantively and positively correlate with ground-based aerosol and $PM_{2.5}$ measurements (Bibi et al. 2015; Bright and Gueymard 2019; Chu et al. 2016), and AOD is often used as a predictor of ambient $PM_{2.5}$ exposures with locally and temporally calibrated prediction functions (Chen et al. 2022; Fu et al. 2018; Yang et al. 2019).

To create a globally consistent and transparent scale, we use a global linear model to relate our AOD estimates to existing global estimates of $PM_{2.5}$. Specifically, we relate the cell-specific annual average AOD values we derived to global gridded estimates of surface $PM_{2.5}$ concentration derived based on models that use satellite-based AOD measures as inputs and ground-based $PM_{2.5}$ data for calibration and model validation (Hammer et al. 2020). Regressing the $PM_{2.5}$ values from Hammer et al. (2020) on our AOD measures, we find that a bivariate linear model with subregion fixed effects provides a reasonable global fit with an R^2 of 0.78. We obtain similar fit and estimates when we restrict the data to only populated cells or when we use all available cells, and higher polynomial orders do not significantly improve the fit.

In our results discussions, we also compare the AOD-transformed $PM_{2.5}$ measures to the WHO interim targets for particulate matter air pollution.[2] These targets are used as guidelines for classifying the severity of $PM_{2.5}$ exposures. The WHO guideline recommends lowering annual average exposure levels to less than 35 $\mu g/m^3$, 25 $\mu g/m^3$, 15 $\mu g/m^3$, and 10 $\mu g/m^3$ as interim targets 1, 2, 3, and 4.

3 Within and across country distributions of air pollution by aerosols

Combining global AOD measures and population data, we present in this section the overall population-weighted global distribution of air pollution by aerosols. In contrast to prior studies on global population-based inequality in ambient air pollution, which have focused on comparing means across regions and countries (Shaddick et al. 2018; Van Donkelaar et al. 2021;

2. The report can be found here https://www.who.int/publications/i/item/9789240034228

Van Donkelaar et al. 2016), we study global inequalities based by conducting comparisons within and across region as well as countries.

3.1 Global distributions

Overall global distribution Figure **??** presents histograms for the global relative distribution of air pollution by aerosols, measured in units of excess aerosol burden. The country-based result in Panel (a) shows the country-aggregate population weighted distribution of country-specific within-country population-weighted means. The cell-based distribution in Panel (b) uses cell-specific results, weighted by cell-specific population estimates.[3]

Panel (a)'s country-level distribution of global excess aerosol burden ranges from -0.81 to 1.18, and has an 80^{th} percentile that is 1.44 times larger relative to its 20^{th} percentile. In contrast, Panel (b)'s cell level distribution of global excess aerosol burden ranges from approximately -1.0 to 10.06, and has an 80^{th} percentile that is 3.62 times more exposed than the 20^{th} percentile. Comparisons between the panels demonstrate that country-level information, even when properly weighted by within country distributions, masks the inequalities across cells within countries. Our analysis in the following sections focus on population-weighted cell-based distributions.

Global dispersion map Figure 1 presents a global map of the relative distribution of air pollution by aerosols in Panel (a). The map matches cell-specific AOD to cell locations. The colors correspond to levels of global excess aerosol burdens—darker shades of green (red) represent greater magnitudes of negative (positive) excess burdens.

The map shows that Asia and Africa have relatively higher levels of air pollution by aerosols. Focusing on countries, India, China, and Pakistan stand out as large countries with areas experiencing high levels of excess aerosol burdens. In contrast, Australia, Mexico, and Argentina are also large economies, but have relatively lower levels of excess aerosol burdens. Additionally, there are variations in the within-country heterogeneities of exposures. For example, locations in the southeastern and northwestern regions of China have high excess burdens, but areas in northern and southwestern China have relative lower levels of excess burdens. In contrast, countries within Western Europe and North America tend to have limited variations concentrated around lower levels of excess burdens.

3. In Appendix Figure E.7, we present un-weighted histograms.

While the world map provides a useful visualization of the global dispersion of air pollution, it does not show the relative population shares facing these heterogeneous burdens across locations.

Population-weighted distributions across continents In Panel (b) of Figure 1, we present continent-specific air pollution distributions that combine the distributions of population and excess aerosol burdens across cells.

Comparing continents at the extremes, the average individual in Asia is 3.32 times more exposed to air pollution by aerosols than the average individual in Oceania. Asia and Oceania have average excess burdens of 0.26 ($\approx$ 29.10 $\mu g/m^3$ of $PM_{2.5}$) and -0.63 ($\approx$ 8.76 $\mu g/m^3$ of $PM_{2.5}$). This means that Asia's and Oceania's global shares of air pollution by aerosols are 26% larger and 63% smaller than their global population shares, respectively.

Africa has the second highest mean exposure with a approximate average $PM_{2.5}$ value of 19.91 $\mu g/m^3$, followed by Europe and the Americas at 14.32 $\mu g/m^3$ and 12.11 $\mu g/m^3$. Oceania is the only continent with average $PM_{2.5}$ reaching WHO interim target 4, which suggests that a considerable share of the world lives in places where air pollution by aerosol exposures are above recommended healthy condition levels.

In addition to the means, the Panel (b) of Figure 1 also shows heterogeneities in the population-weighted dispersion of excess aerosol burdens within each continent. The Americas, Europe, and Oceania have distributions with relatively limited variabilities. Europe is the most equal continent in the world where population at the 80^{th} percentile of excess aerosol burden are only 28% more exposed than those at the 20^{th} percentile. In contrast, distributions in Africa and Asia are more dispersed. Populations at the 80^{th} percentile of the aerosol distribution are 141% and 109% more exposed than population at the 20^{th} percentile in Africa and Asia, respectively. Further at the tails, the exposure faced by populations at the 90^{th} percentile of the aerosol distribution are 227% and 185% higher than those at the 10^{th} percentile in Africa and Asia, respectively.

3.2 Distributions across and within regions and countries

In this section, we decompose the global air pollution by aerosol distribution into sub-continental region- and nation-specific components. We present the results in continent-specific Figures 3 to 4. In each figure, Panel (a) presents air pollution by aerosol distributions by sub-continental

group (e.g., Northern Africa, East Asia), and Panel (b) highlights the 20^{th} and 80^{th} percentiles and means of country-specific distributions. Both results are based on population-weighted cell-level results.

There are substantial differences in means and variabilities across sub-continental regions. In terms of means, Eastern Asia has the highest mean AOD of 0.66 ($\approx 33.68\,\mu g/m^3$ of $PM_{2.5}$), which is just below WHO interim target 1. Australia and New Zealand have the lowest mean AOD of 0.11 ($\approx 7.65\,\mu g/m^3$ of $PM_{2.5}$), which has reached WHO interim target 4. In terms of variabilities, the ratios of exposure for populations at the 80^{th} to 20^{th} percentiles for sub-continental regions range between 1.02 to 3.08, and the 90^{th} to 10^{th} percentile ratios range between 1.06 to 4.31.

Inequalities within Africa Figure 3 shows air pollution by aerosol distributions across cells in the Eastern, Middle, Northern, Southern, and Western Africa regions as well as the variation in cell-level measurments within the countries that fall under these regions. Results show substantial heterogeneities in within-region aerosol exposures.

Western Africa has the highest average annual AOD at 0.51 ($\approx 26\,\mu g/m^3$ of $PM_{2.5}$), almost reaching WHO interim target 2. Southern Africa has the lowest average annual AOD at 0.14 ($\approx 9.05\,\mu g/m^3$ of $PM_{2.5}$), which exceeds WHO interim target 4.

The most populous African country, Nigeria, has an annual average AOD of 0.56 ($\approx 28.98\,\mu g/m^3$ of $PM_{2.5}$), which is behind WHO interim target 2. Nigeria's average exposure level corresponds to a global excess aerosol burden of 0.24, meaning that Nigeria's global share of air pollution by aerosols is 24% larger than its population share. Exposure inequalities are significant within Nigeria—Nigerian population at the 80^{th} (90^{th}) percentile of aerosol distribution are 77% (106%) more exposed than those at the 20^{th} (10^{th}) percentile. One of the least populous countries in Africa, Sao Tome and Principe, has an average annual AOD of 0.47 ($\approx 24.65\,\mu g/m^3$ of $PM_{2.5}$), just passing WHO interim target 2. In contrast to Nigeria, relative population exposure percentiles are close to 1 due to the small size of the country.

At 0.66 ($\approx 35.18\,\mu g/m^3$ of $PM_{2.5}$), the Congolese population faces the highest average annual AOD in Africa, which lags behind WHO interim target 1. Congo's global share of air pollution by aerosols is 53% larger than its population share. Exposure inequalities are limited within Congo—Congolese population at the 80^{th} (90^{th}) percentile of aerosol distribution are 15% (22%) more exposed than those at the 20^{th} (10^{th}) percentile. In contrast, at 0.09

($\approx 6.42\,\mu g/m^3$ of $PM_{2.5}$), the population in Lesotho faces the lowest average annual AOD average in Africa, which significantly surpasses WHO interim target 4. Lesotho's global share of air pollution by aerosols is 81% smaller than its population share. Exposure inequalities are limited except at the far tails within Lesotho— the Lesothoan population at the 80^{th} (90^{th}) percentile of aerosol distribution are 0% (40%) more exposed than those at the 20^{th} (10^{th}) percentile.

Inequalities within Americas Figure 5 shows air pollution by aerosol distributions for countries in the Caribbean, Central America, Northern America, and South America. Compared to Africa and Asia, distributions in regions in the Americas have limited variabilities.

South America has the highest average annual AOD at 0.22 ($\approx 12.93\,\mu g/m^3$ of $PM_{2.5}$). Central America has the lowest average annual AOD at 0.19 ($\approx 11.65\,\mu g/m^3$ of $PM_{2.5}$). All regions in the Americas, on average, have reached WHO interim targets 3.

The most populous country in the Americas, the United States of America, has an annual average AOD of 0.19 ($\approx 11.67\,\mu g/m^3$ of $PM_{2.5}$), close to reach WHO interim target 4. The US's average exposure level corresponds to a global excess aerosol burden of -0.56, meaning that the US's global share of air pollution by aerosols is 56% smaller than its population share. Exposure inequalities are important but limited in the US—Americans population at the 80^{th} (90^{th}) percentile of aerosol distribution are 36% (71%) more exposed than those at the 20^{th} (10^{th}) percentile. One of the least populous countries in the Americas, Saint Lucia, has an average annual AOD of 0.21 ($\approx 12.49\,\mu g/m^3$ of $PM_{2.5}$). Relative population exposure percentiles is equal to 1 in Saint Lucia.

At 0.34 ($\approx 18.55\,\mu g/m^3$ of $PM_{2.5}$), Colombian population face the highest average annual AOD in the Americas, which is behind WHO interim target 3. Colombia's global share of air pollution by aerosols is 24% smaller than its population share. Exposure inequalities are important but limited within Colombia—Colombian population at the 80^{th} (90^{th}) percentile of aerosol distribution are 28% (55%) more exposed than those at the 20^{th} (10^{th}) percentile. In contrast, at 0.10 ($\approx 7.27\,\mu g/m^3$ of $PM_{2.5}$), population in Chile face the lowest average annual AOD in the Americas, which achieves WHO interim target 4. Chile's global share of air pollution by aerosols is 77% smaller than its population share.

Inequalities within Asia Figure 2 shows air pollution by aerosol distributions for countries in Central, Eastern, Southeastern, Southern, and Western Asia. Results show substantial heterogeneities in within-region and within-country aerosol exposures.

Eastern Asia has both the highest average levels of exposure and variabilities in exposures, and Central Asian has the lowest. Eastern Asia has an average annual AOD of 0.66 ($\approx$ 33.68 $\mu g/m^3$ of $PM_{2.5}$). Eastern Asian population at the 80^{th} percentile of aerosol distribution are 158% more exposed than those at the 20^{th} percentile, and its population at the 90^{th} percentile of aerosol distribution are 223% more exposed than those at the 10^{th} percentile. Central Asia has an average annual AOD of 0.36 ($\approx$ 19.49 $\mu g/m^3$ of $PM_{2.5}$), reaching WHO interim target 3. Central Asia's population at the 80^{th} (90^{th}) percentile of aerosol distribution are 64% (110%) more exposed than those at the 20^{th} (10^{th}) percentile.

The most populous Asian country, China, has an annual average AOD of 0.7 ($\approx$ 35.58 $\mu g/m^3$ of $PM_{2.5}$), which is behind WHO interim target 1, indicating very hazardous levels of average air pollution by aerosols. China's average exposure level corresponds to a global excess aerosol burden of 0.55, meaning that China's global share of air pollution by aerosols is 55% larger than its population share. Exposure inequalities are large within China— the Chinese population at the 80^{th} (90^{th}) percentile of aerosol distribution are 111% (216%) more exposed than those at the 20^{th} (10^{th}) percentile. One of the least populous countries in Asia, Qatar, has an average annual AOD of 0.60, which is similar to the level in China. Relative population exposure percentiles are equal to 1 due to the geographical confines of Qatar.

In Asia, populations in Kuwait and East Timor are at the opposite ends of the air pollution by aerosol exposure spectrum. Both countries' relative within country exposure percentiles are close to 1. At 0.99 ($\approx$ 49.06 $\mu g/m^3$ of $PM_{2.5}$), the Kuwaiti population faces the highest average annual AOD in Asia, which is substantially behind WHO interim target 1. In contrast, at 0.17 ($\approx$ 10.74 $\mu g/m^3$ of $PM_{2.5}$), East Timor population have the lowest average annual AOD in Asia, almost reaching WHO interim target 4. In terms of global excess aerosol burdens, Kuwait's share of global ambient air pollution by aerosol is 118% larger than its global population share, and East Timor's air pollution share is 60% less than its population share.

Inequalities within Europe Figure 4 shows air pollution by aerosol distributions for countries in Eastern, Northern, Southern, and Western Europe. Compared to Africa and Asia, distributions in European regions have limited variabilities.

Eastern Europe has the highest average annual AOD at 0.28 ($\approx 15.53\,\mu g/m^3$ of $PM_{2.5}$), just reaching WHO interim target 3. Southern Europe has the lowest average annual AOD at 0.21 ($\approx 12.51\,\mu g/m^3$ of $PM_{2.5}$), exceeding interim target 3.

The most populous European country, Russia, has an annual average AOD of 0.29 ($\approx 16.39\,\mu g/m^3$ of $PM_{2.5}$), which is behind WHO interim target 3. Russia's average exposure level corresponds to a global excess aerosol burden of -0.34, meaning that Russia's global share of air pollution by aerosols is 34% smaller than its population share. Exposure inequalities are significant within Russia—Russian population at the 80^{th} (90^{th}) percentile of aerosol distribution are 67% (130%) more exposed than those at the 20^{th} (10^{th}) percentile. One of the least populous countries in Europe, Iceland, has an average annual AOD of 0.21 ($\approx 12.68\,\mu g/m^3$ of $PM_{2.5}$), close to reaching WHO interim target 4. Despite its limited population, there are exposure variabilities in Iceland due to its large geography—Icelandic population at the 80^{th} (90^{th}) percentile of aerosol distribution are 39% (49%) more exposed than those at the 20^{th} (10^{th}) percentile.

Russia has the highest average annual AOD in Europe. In contrast, at 0.15, population in Norway face the lowest average annual AOD in Europe. Norway's global share of air pollution by aerosols is 65% smaller than its population share. Exposure inequalities are limited but present in Norway—Norwegian population at the 80^{th} (90^{th}) percentile of aerosol distribution are 21% (31%) more exposed than those at the 20^{th} (10^{th}) percentile.

Inequalities within Oceania Figure 6 shows air pollution by aerosol distributions for countries in Oceania, which has a small number of countries dominated in population by Australia, Papua New Guinea, and New Zealand. Melanesia has the highest average annual AOD at 0.20 ($\approx 12\,\mu g/m^3$ of $PM_{2.5}$), which is just above WHO interim target 4. As a region, Australia and New Zealand have the lowest average annual AOD at 0.11 ($\approx 7.65\,\mu g/m^3$ of $PM_{2.5}$), which exceeds WHO interim target 4. Compared to the rest of the world, all populated cells in Oceania have relative low levels of air pollution by aerosol exposures.

4 Air pollution by aerosols and GDP per capita

In this section we analyze the national and subnational level relationships between air pollution by aerosols, as measured by AOD, and economic development, as measured by GDP

(PPP-adjusted) per capita (Gennaioli et al. 2013; Kummu, Taka, and Guillaume 2018). Specifically, we regress GDP per capita on global excess aerosol burdens at the national and subnational levels. We allow for homogeneous or heterogeneous bivariate relationships across continents and account for continental and sub-continental regional fixed effects. We present our results in Table 1 and Figure 7. Results from various estimations jointly inform the direction and magnitude of the GDP and aerosol association globally and for each continent, and explain whether the findings are due to across region—variations in regional means—or within region—variations in national and subnational values conditional on regional means—associations.

Global association In this section, we analyze the global association between air pollution by aerosols and GDP per capita. We find a strong negative association using both national and subnational data, which are largely explained by associations of continental means.

In Table 1, the global country-level result from column (1) of Panel (a) presents the slope from a bivariate regression of excess aerosol burden on GDP per capita, treating each country with equal weight. We find an estimated slope of -0.075 (s.e. 0.018). This means that a doubling of GDP per capita is associated with a reduction of a country's excess aerosol burden by 7.5 percentage points—this is a 7.5 percentage points reduction in the percentage deviation between the country-specific AOD value and the global mean. In column (2) of Panel (a), we incorporate country-specific weights, which leads to a doubling of the slope coefficient to -0.144 (s.e. 0.023). This means that countries with larger population tend to have a stronger negative aerosol to GDP associations.

Given the large heterogeneities in within country air pollution by aerosol distribution as well as large heterogeneities in economic development within countries, patterns based on national aggregates might differ from subnational results. In columns (4) and (5) of Panel (a), we estimate the same relationships as in columns (1) and (2) of Panel (a), but using more granular subnational data. We find similar negative slopes of -0.083 (s.e. 0.007) and -0.118 (s.e. 0.008) from the equal weight and population-weighted results.

In both national and subnational regressions, variations in global GDP per capita explain a significant proportion of variabilities in excess aerosol burden. From the national results, for the unweighted and weighted regressions, 9% and 19% of the variabilities in air pollution by aerosols are accounted for by variabilities in GDP per capita, respectively. For subnational

results, the shares of variabilities explained are still substantially at 4% and 5% for the unweighted and weighted regressions, respectively.

There are large differences in mean levels of economic development and air pollution across continents, as is visible from the differentiated concentration of countries from each continent along the x-axis and y-axis in Figure 7. Specifically, Africa and Asia populate all the quadrants of the figure. In contrast, Europe, the Americas, and Oceania are concentrated in the lower quadrants with dispersion in economic activities but limited variations in air pollution. We analyze the extent to which the air pollution by aerosol and GDP per capita association just documented is explained by the association in continental-level means. We accomplish this in columns (3) and (6) of Panel (a) by introducing continental-level fixed effects to the weighted national and subnational regressions from columns (2) and (5). Globally, we continue to find that higher GDP per capita is associated with less aerosol exposures, but the relationship is significantly weakened—the national-level slope estimate is -0.037 (0.024) and the subnational-level slope estimate is -0.009 (0.009). This result indicates that continental-level mean correlations explain most of the global aerosol and GDP correlation.

Continent-specific Associations In this section, we allow for heterogeneous associations between air pollution by aerosols and GDP per capita in each continent. The previous section assumed that this association is homogeneous across all countries, but depending on the predominant stage that countries in a continent are undergoing, the relationship between air pollution and economic development might differ. For example, in developing economies like India, it may be the case that having higher income is connected to living in areas that are more polluted whereas in developed economies like Germany, higher wealth instead affords one the ability to live in a less polluted area. In Panel (b) of Table 1, we present estimates for continent-specific associations by allowing for both continent-specific fixed effects as well as continent-specific slopes.

Focusing on the national and subnational population-weighted results in columns (2) and (5) in Panel (b), we find significant variations in the magnitudes of aerosol and GDP association by continents. We find positive slopes for Africa with estimates of 0.023 (s.e. 0.054) and 0.052 (s.e. 0.020) using national and subnational data. The subnational estimate shows that a doubling of GDP per capita for a subnational unit in Africa is associated with a 5.2 percentage points increase in the percentage deviation between the subnational AOD value the the

global mean, meaning that a national increase in GDP per capita is actually associated with an exacerbation of pollution inequality across the continent. In contrast, we find significant negative associations in Europe, the Americas, and Oceania, with slopes estimates of -0.016 (s.e. 0.006), -0.019 (s.e. 0.005), and -0.071 (s.e. 0.006) from the subnational results. These indicate that in these areas, higher levels of economic development is associated with lower levels of air pollution by aerosol. Our results for Asia are statistically insignificant, indicating a lack of relationship between economic development and air pollution at the continental level across Asia. We present continent-specific scatter plots using national and subnational data in Appendix Figure E.10.

In columns (3) and (6) of Panel (b), we continue to analyze continent-specific correlations after adding in sub-continental regional group fixed effects. We previously documented significant heterogeneities in sub-continental regional air pollution by aerosol distributions, especially in Asia and Africa. Within each continent, regional average associations between economic development and air pollution could reinforce or mask the GDP and aerosol associations across subnational economic units within each region.

Including subcontinental regional fixed effects and focusing on the subnational results from column (6), our results for Africa, the Americas, Oceania, and Asia are in the same direction but stronger compared to results from column (5) without the subcontinental regional fixed effects. Specifically, we find a positive slope estimate of 0.088 (s.e. 0.023) for Africa. For the Americas and Oceania, we find slope estimates of -0.022 (0.008) and -0.077 (s.e. 0.009). For Asia, the insignificant negative association from column (5) is strengthened to a negative slope of -0.099 (s.e. 0.022)—this means that a doubling of GDP per capita for a subnational unit in Asia is associated with a 9.9 percentage points reduction in the percentage deviation between the subnational AOD value the the global mean. The strengthening of the magnitudes of the slope estimates indicates that the association between GDP and aerosols across subcontinental regions and within subcontinental regions tend to be in opposite directions, especially for Asia.

In contrast to the other continents, in Europe, the slope switches signs after including subcontinental regional fixed effects, column (6) reports a positive slope of 0.053 (s.e. 0.008). This means that looking only at within region variations in GDP and aerosols, a doubling of GDP per capita for a subnational unit in Europe is associated with a 5.3 percentage points increase in the percentage deviation between the subnational AOD value the the global mean. The switch in the sign of the slope indicates that in Europe, regions with higher average GDP per capita

tend to have lower average levels of air pollution by aerosols, but controlling for regional means, subnational units with higher GDP tend to have higher air pollution.

5 Discussion and Conclusion

In this paper, using data from around 2010—the most recent year around which reliable granular global population, air pollution by aerosol, and GDP per capita data are jointly available—we document the global relative distribution of air pollution by aerosols across and within regions and countries, and we analyze the global and continental associations between air pollution by aerosol and GDP per capita.

Our focus on population-weighted distribution of air pollution contrasts with much of the focus in the scientific literature on climate change, which focuses largely on the distribution of climatic burden across locations, with relatively little attention to the relative population exposures to climatic burdens across AND within locations (Mehta et al. 2016; Tian et al. 2023). This paper follows recent works that have combined global gridded population with air pollution data (Shaddick et al. 2018; Van Donkelaar et al. 2021; Van Donkelaar et al. 2016), which have generally focused on analyzing variabilities in regional and national means as well as aggregate distributions for large supra-national groupings. In contrast, our population weighted analysis decomposes the overall global population-weighted air pollution by aerosol distribution into both across and within region and country components.

The results suggest the existence of pollution inequalities across locations over the globe, with Asian population facing the highest average exposure, followed by populations in Africa, Europe, the Americas, and Oceania. At the continental extremes, Asia's global shares of air pollution by aerosols is 26% larger than its population share, but Oceania's is 63% smaller. We find that the Americas, Europe, and Oceania have distributions with relatively limited variabilities. Europe is the most equal continent in the world with population at the 80^{th} percentile of air pollution by aerosol exposure only 28% more exposed than those at the 20^{th} percentile. In contrast, in Africa and Asia, populations at the 80^{th} percentile of the air pollution by aerosol distribution are 141% and 109% more exposed than population at the 20^{th} percentile, respectively. Across subcontinental regions, the percentage increases in exposure between the 80^{th} and 20^{th} percentiles range from 2% to 208%. This range widens further to from 0% to 359% when we condition further on within country air pollution by aerosol distributions.

The paper also provides evidence about the relationship between pollution burden and economic activity measured by GDP per capita. Overall, we find a strong negative global correlation. In particular, using subnational population-weighted data, we find that a doubling of GDP per capita is associated with a 11.8 percentage points reduction in the percentage deviation between the a subnational unit's population-weighted air pollution by aerosol level and the global population-weighted mean. The association is significantly weakened when continental fixed effects are included, which means the global association is largely explained by correlation between continental-level mean GDP per capita and air pollution by aerosol.

Furthermore, we analyze the GDP and air pollution relationship within each continent. Exploiting variabilities in subnational data and controlling for aggregate regional variabilities through subcontinental regional fixed effects, we find a positive association between air pollution by aerosols and GDP per capita in Africa and Europe, but negative association in the Americas, Asia, and Oceania. Specifically, we find the strongest negative association in Asia and the strongest positive association in Africa—a doubling of GDP per capita for a subnational unit in Asia and Africa are associated with a 9.9 percentage points reduction and 8.8 percentage points increase in the percentage deviation between the a subnational unit's population-weighted air pollution by aerosol level and the global population-weighted mean, respectively.

There are limitations to our analysis. First, our analysis is centered around one year. While it would be of great interest to compare changes over time, the population census and register data we rely on are from different years centered around 2010 (CIESIN Columbia University 2018), and the subnational GDP dataset we use only has data up to 2010 (Gennaioli et al. 2013) and requires extrapolation to extend the dataset to later years (Kummu, Taka, and Guillaume 2018). Second there are trade-offs between the granularity of cells at which we merge population and air pollution by aerosol data and the precision and availability of cell-specific averages. We use $1^\circ \times 1^\circ$ longitude–latitude grid, which reduces the precision of our population-weighted air pollution by aerosol estimates for smaller countries, but improves the number of raw satellite-based measurements we can draw on to measure air pollution by aerosol exposures for each cell. Third, rather than using climate models to transform AOD to particulate matter measurements (Hammer et al. 2020), for transparency and to reduce the number of intermediating estimation and approximation layers between raw satellite data measurements and inputs for empirical analysis, we use AOD-based measures directly to assess the global

distribution of air pollution by aerosols. We present results in AOD levels and in units of relative global excess aerosol burdens. Given the importance of particulate matter to human health, we also provide approximately translated $PM_{2.5}$ values to facilitate the interpretation of our AOD-based results.

References

Bibi, Humera, Khan Alam, Farrukh Chishtie, Samina Bibi, Imran Shahid, and Thomas Blaschke. 2015. "Intercomparison of MODIS, MISR, OMI, and CALIPSO Aerosol Optical Depth Retrievals for Four Locations on the Indo-Gangetic Plains and Validation Against AERONET Data." *Atmospheric Environment* 111 (June 1, 2015): 113–126. https://doi.org/10.1016/j.atmosenv.2015.04.013.

Brabhukumr, Ajith, Prabhjot Malhi, Khaiwal Ravindra, and PVM Lakshmi. 2020. "Exposure to Household Air Pollution During First 3 Years of Life and Iq Level Among 6–8-Year-Old Children in India–a Cross-Sectional Study." *Science of The Total Environment* 709:135110.

Bright, Jamie M., and Christian A. Gueymard. 2019. "Climate-Specific and Global Validation of MODIS Aqua and Terra Aerosol Optical Depth at 452 AERONET Stations." *Solar Energy* 183 (May 1, 2019): 594–605. https://doi.org/10.1016/j.solener.2019.03.043.

Chen, Youliang, Dan Li, Hamed Karimian, Shiteng Wang, and Shuwei Fang. 2022. "The Relationship Between Air Quality and MODIS Aerosol Optical Depth in Major Cities of the Yangtze River Delta." *Chemosphere* 308 (Pt 2): 136301. https://doi.org/10.1016/j.chemosphere.2022.136301.

Chu, Yuanyuan, Yisi Liu, Xiangyu Li, Zhiyong Liu, Hanson Lu, Yuanan Lu, Zongfu Mao, et al. 2016. "A Review on Predicting Ground PM2.5 Concentration Using Satellite Aerosol Optical Depth." *Atmosphere* 7, no. 10 (October): 129. https://doi.org/10.3390/atmos7100129.

CIESIN Columbia University. 2018. *Gridded Population of the World, Version 4 (GPWv4): Basic Demographic Characteristics, Revision 11.* Palisades, New York. https://doi.org/10.7927/H46M34XX.

Cornillon, P., J. Gallagher, and T. Sgouros. 2003. "OPeNDAP: Accessing Data in a Distributed, Heterogeneous Environment." *Data Science Journal* 2:164–174. https://doi.org/10.2481/dsj.2.164.

Fisher, Samantha, David C Bellinger, Maureen L Cropper, Pushpam Kumar, Agnes Binagwaho, Juliette Biao Koudenoukpo, Yongjoon Park, et al. 2021. "Air Pollution and Development in Africa: Impacts on Health, the Economy, and Human Capital." *The Lancet Planetary Health* 5 (10): e681–e688.

Fu, Disong, Xiangao Xia, Jun Wang, Xiaoling Zhang, Xiaojing Li, and Jianzhong Liu. 2018. "Synergy of AERONET and MODIS AOD Products in the Estimation of PM2.5 Concentrations in Beijing." *Scientific Reports* 8, no. 1 (July 5, 2018): 10174. https://doi.org/10.1038/s41598-018-28535-2.

Fu, Shihe, V Brian Viard, and Peng Zhang. 2021. "Air Pollution and Manufacturing Firm Productivity: Nationwide Estimates for China." *The Economic Journal* 131 (640): 3241–3273.

Gakidou, Emmanuela, Ashkan Afshin, Amanuel Alemu Abajobir, Kalkidan Hassen Abate, Cristiana Abbafati, Kaja M Abbas, Foad Abd-Allah, et al. 2017. "Global, Regional, and National Comparative Risk Assessment of 84 Behavioural, Environmental and Occupational, and Metabolic Risks or Clusters of Risks, 1990–2016: A Systematic Analysis for the Global Burden of Disease Study 2016." *The Lancet* 390 (10100): 1345–1422.

Gennaioli, Nicola, Rafael La Porta, Florencio Lopez-de-Silanes, and Andrei Shleifer. 2013. "Human Capital and Regional Development." *The Quarterly Journal of Economics* 128, no. 1 (February 1, 2013): 105–164. https://doi.org/10.1093/qje/qjs050.

Hammer, Melanie S, Aaron van Donkelaar, Chi Li, Alexei Lyapustin, Andrew M Sayer, N Christina Hsu, Robert C Levy, et al. 2020. "Global Estimates and Long-Term Trends of Fine Particulate Matter Concentrations (1998–2018)." *Environmental Science & Technology* 54 (13): 7879–7890.

Holben, B. N., T. F. Eck, I. Slutsker, D. Tanré, J. P. Buis, A. Setzer, E. Vermote, et al. 1998. "AERONET—A Federated Instrument Network and Data Archive for Aerosol Characterization." *Remote Sensing of Environment* 66, no. 1 (October 1, 1998): 1–16. https://doi.org/10.1016/S0034-4257(98)00031-5.

Jacobson, Mark Z. 2002. *Atmospheric Pollution: History, Science, and Regulation.* Cambridge: Cambridge University Press. https://doi.org/10.1017/CBO9780511802287.

Kummu, Matti, Maija Taka, and Joseph HA Guillaume. 2018. "Gridded Global Datasets for Gross Domestic Product and Human Development Index Over 1990–2015." *Scientific data* 5 (1): 1–15.

Lenoble, Jacqueline, Lorraine Remer, and Didier Tanre. 2013. *Aerosol Remote Sensing*. Springer Science & Business Media, February 11, 2013.

Mehta, Manu, Ritu Singh, Ankit Singh, Narendra Singh, and Anshumali. 2016. "Recent Global Aerosol Optical Depth Variations and Trends — a Comparative Study Using MODIS and MISR Level 3 Datasets." *Remote Sensing of Environment* 181 (August 1, 2016): 137–150. https://doi.org/10.1016/j.rse.2016.04.004.

NASA Earth Observatory. 2024. "Aerosol Optical Depth." Aerosol Optical Depth. https://earthobservatory.nasa.gov/global-maps/MODAL2_M_AER_OD.

Odo, Daniel B, Ian A Yang, Sagnik Dey, Melanie S Hammer, Aaron van Donkelaar, Randall V Martin, Guang-Hui Dong, et al. 2023. "A Cross-Sectional Analysis of Long-Term Exposure to Ambient Air Pollution and Cognitive Development in Children Aged 3–4 Years Living in 12 Low-and Middle-Income Countries." *Environmental Pollution* 318:120916.

Pirlea, Florina, and Wendy Ven-dee Huang. 2019. "The Global Distribution of Air Pollution," September 12, 2019. https://datatopics.worldbank.org/world-development-indicators/stories/the-global-distribution-of-air-pollution.html.

Shaddick, Gavin, Matthew L Thomas, Heresh Amini, David Broday, Aaron Cohen, Joseph Frostad, Amelia Green, et al. 2018. "Data Integration for the Assessment of Population Exposure to Ambient Air Pollution for Global Burden of Disease Assessment." *Environmental science & technology* 52 (16): 9069–9078.

Shaddick, Gavin, Matthew L Thomas, Pierpaolo Mudu, Giulia Ruggeri, and Sophie Gumy. 2020. "Half the World's Population Are Exposed to Increasing Air Pollution." *NPJ Climate and Atmospheric Science* 3 (1): 23.

Tian, Xiaomin, Chaoli Tang, Xin Wu, Jie Yang, Fengmei Zhao, and Dong Liu. 2023. "The Global Spatial-Temporal Distribution and EOF Analysis of AOD Based on MODIS Data During 2003–2021." *Atmospheric Environment* 302 (June 1, 2023): 119722. https://doi.org/10.1016/j.atmosenv.2023.119722.

Van Donkelaar, Aaron, Melanie S Hammer, Liam Bindle, Michael Brauer, Jeffery R Brook, Michael J Garay, N Christina Hsu, et al. 2021. "Monthly Global Estimates of Fine Particulate Matter and Their Uncertainty." *Environmental Science & Technology* 55 (22): 15287–15300.

Van Donkelaar, Aaron, Randall V Martin, Michael Brauer, N Christina Hsu, Ralph A Kahn, Robert C Levy, Alexei Lyapustin, et al. 2016. "Global Estimates of Fine Particulate Matter Using a Combined Geophysical-Statistical Method with Information from Satellites, Models, and Monitors." *Environmental science & technology* 50 (7): 3762–3772.

Wang, Qingxin, Dongsheng Du, Siwei Li, Jie Yang, Hao Lin, and Juan Du. 2021. "Comparison of Different Methods of Determining Land Surface Reflectance for AOD Retrieval." *Atmospheric Pollution Research* 12, no. 8 (August 1, 2021): 101143. https://doi.org/10.1016/j.apr.2021.101143.

Xiong, Xiaoxiong, Emily J. Aldoretta, Amit Angal, Tiejun Chang, Xu Geng, Daniel O. Link, Vincent V. Salomonson, et al. 2020. "Terra MODIS: 20 Years of on-Orbit Calibration and Performance." *Journal of Applied Remote Sensing* 14, no. 3 (August): 037501. https://doi.org/10.1117/1.JRS.14.037501.

Yang, Qianqian, Qiangqiang Yuan, Linwei Yue, Tongwen Li, Huanfeng Shen, and Liangpei Zhang. 2019. "The Relationships Between PM2.5 and Aerosol Optical Depth (AOD) in Mainland China: About and Behind the Spatio-Temporal Variations." *Environmental Pollution* 248 (May 1, 2019): 526–535. https://doi.org/10.1016/j.envpol.2019.02.071.

Figure 1: Continental population-weighted distribution of air pollution by aerosols, 2010

(a) 1° cell (1° × 1° longitude–latitude grid) as the unit of observation map

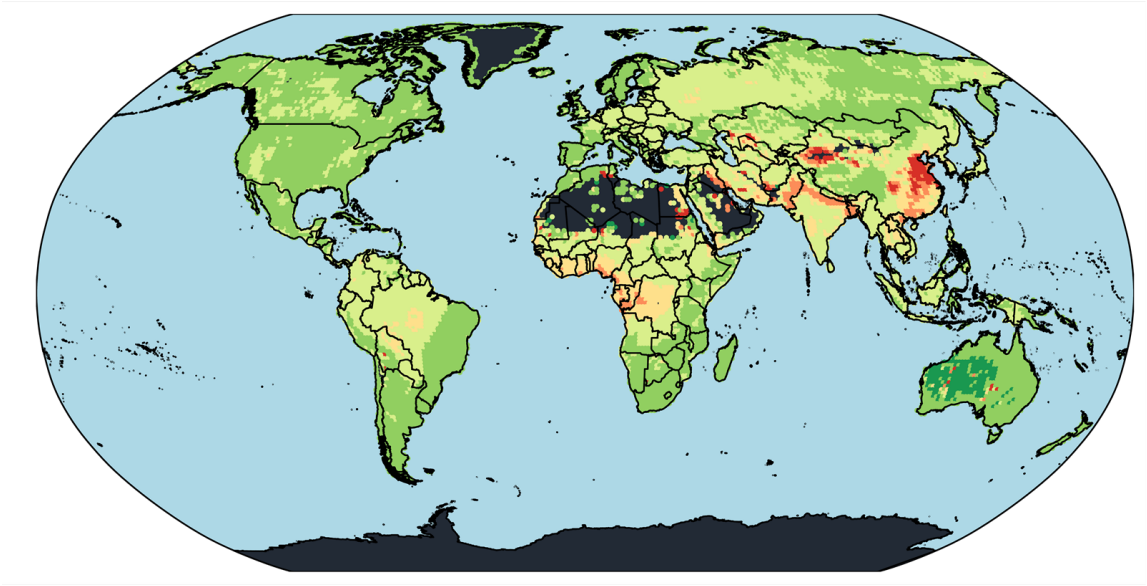

(b) 1° cell as the unit of observation (weighted by cell-population), by regions

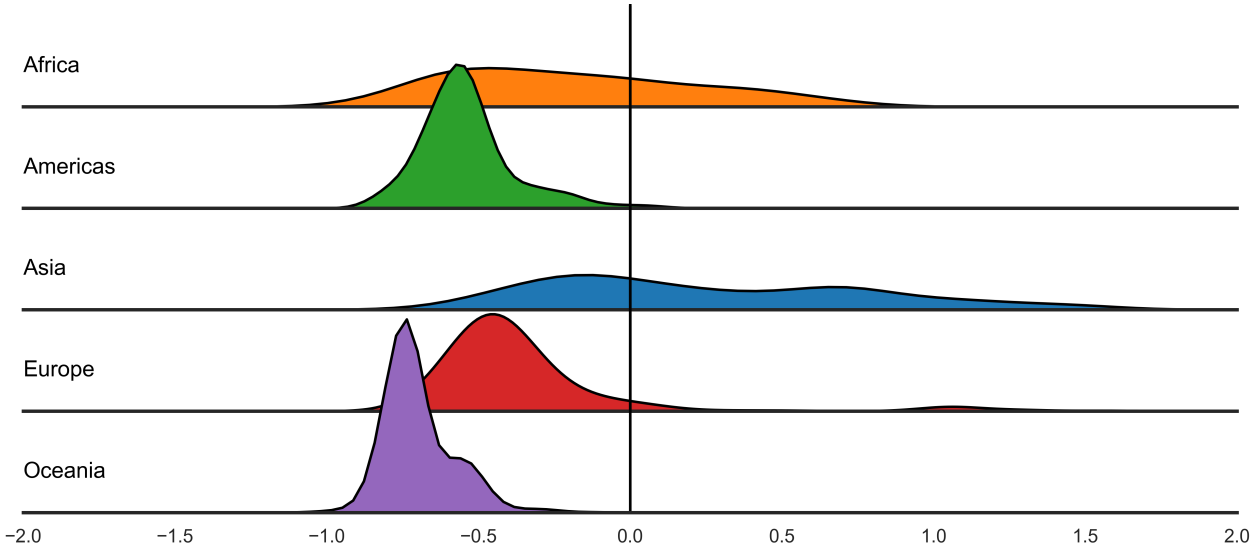

Notes: The panels present the global relative distribution of air pollution by aerosols as measured by Aerosol Optical Depth (AOD). We compute annual average AOD for each 1° cell. The map in Panel (a) matches cell-specific AOD to cell locations. The distribution in Panel (b) uses cell-specific AOD, weighted by cell-specific population estimates. The y-axis in Panel (b) shows cell population weighted density approximations. The colors in Panel (a) and x-axis in Panel (b) correspond to what we call global excess aerosol burden: A value of 0.5 (-0.5) indicates that a cell's AOD measure is 50 percent greater (smaller) than the global weighted mean. In Panel (b), darker shades of green (red) correspond to greater magnitudes of negative (positive) excess burdens.

Figure 2: Asian population-weighted distribution of air pollution by aerosols, 2010

(a) 1° cell as the unit of observation (weighted by cell-population), by sub-regions

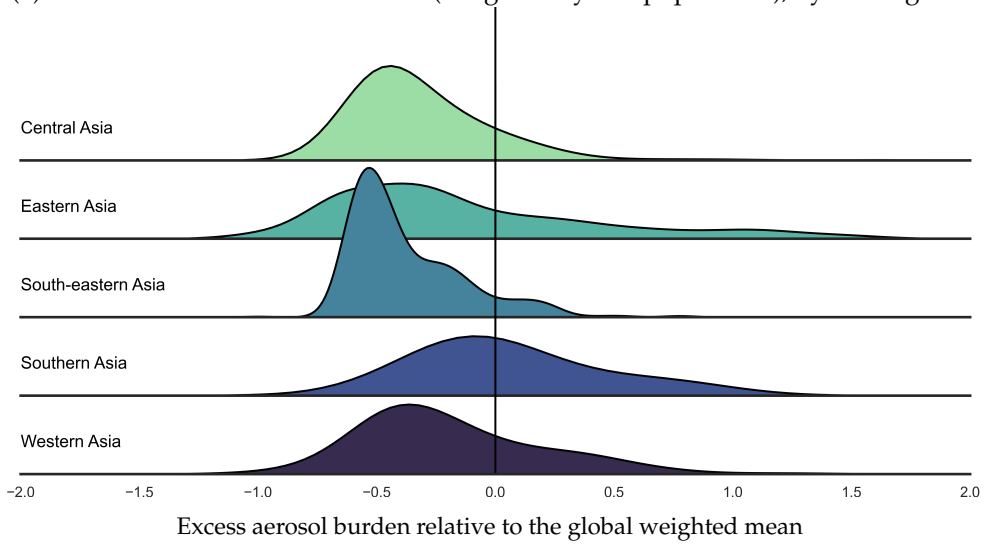

(b) Country-specific distributional ranges: P20 (*left-dot*), mean (*center-dot*), P80 (*right-dot*)

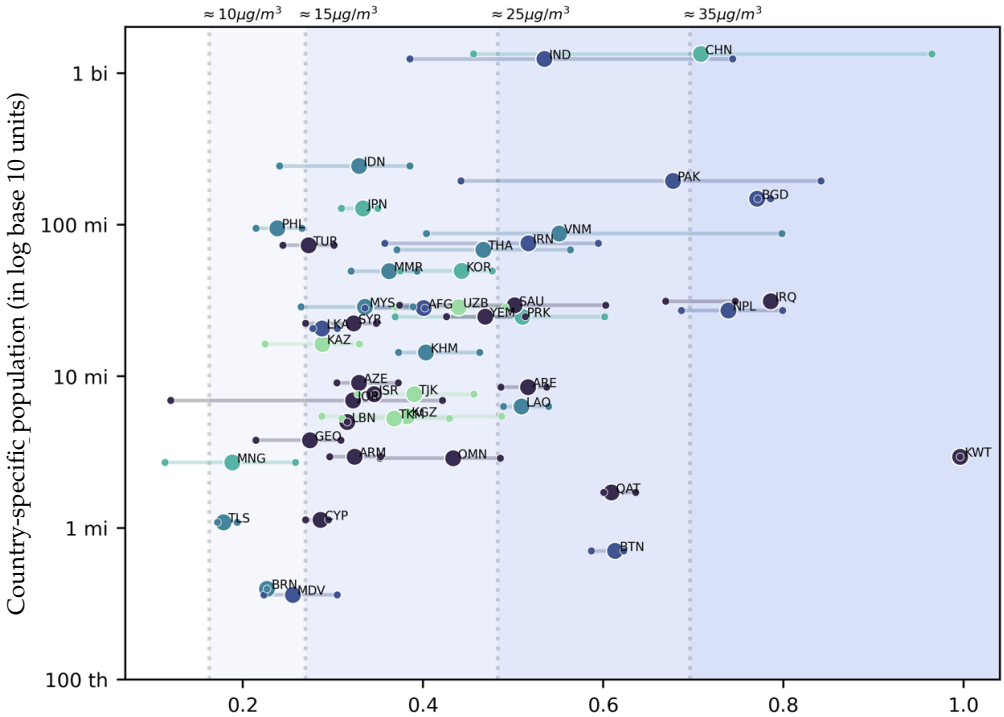

Notes: The panels present the Asian distribution of air pollution by aerosols as measured by Aerosol Optical Depth (AOD). We compute annual average AOD for each 1° cell. Panel (b) lines mark the 20th percentile, mean, and the 80th percentile of a country's AOD distribution, computed based on the distribution of AOD and population across cells corresponding to each country. In Panel (a), the y-axis shows cell population weighted density approximations. The x-axis in Panel (a) corresponds to levels of excess aerosol burden, a value of 0.5 (-0.5) indicates that a cell's AOD measure is 50 percent greater (smaller) than the global weighted mean. The x-axis in Panel (b) is in AOD units and tick-labels show AOD values. The vertical dashed lines corresponding to PM 2.5 thresholds in $\mu g/m^3$ units according to WHO interim targets (ITs). Background color corresponds to the IT ranges, with darker colors indicating lower air quality thresholds.

Figure 3: African population-weighted distribution of air pollution by aerosols, 2010

(a) 1° cell as the unit of observation (weighted by cell-population), by sub-regions

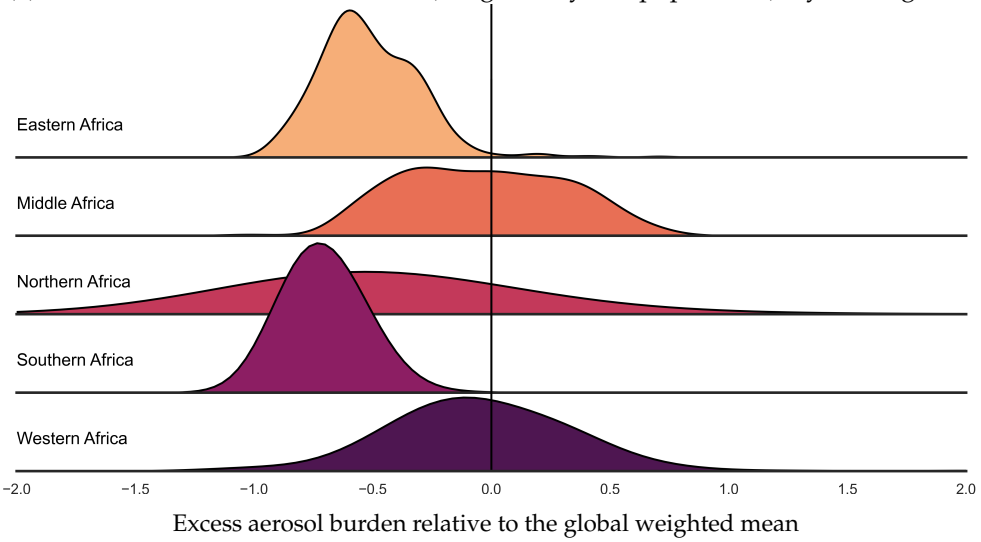

(b) Country-specific distributional ranges: P20 (*left-dot*), mean (*center-dot*), P80 (*right-dot*)

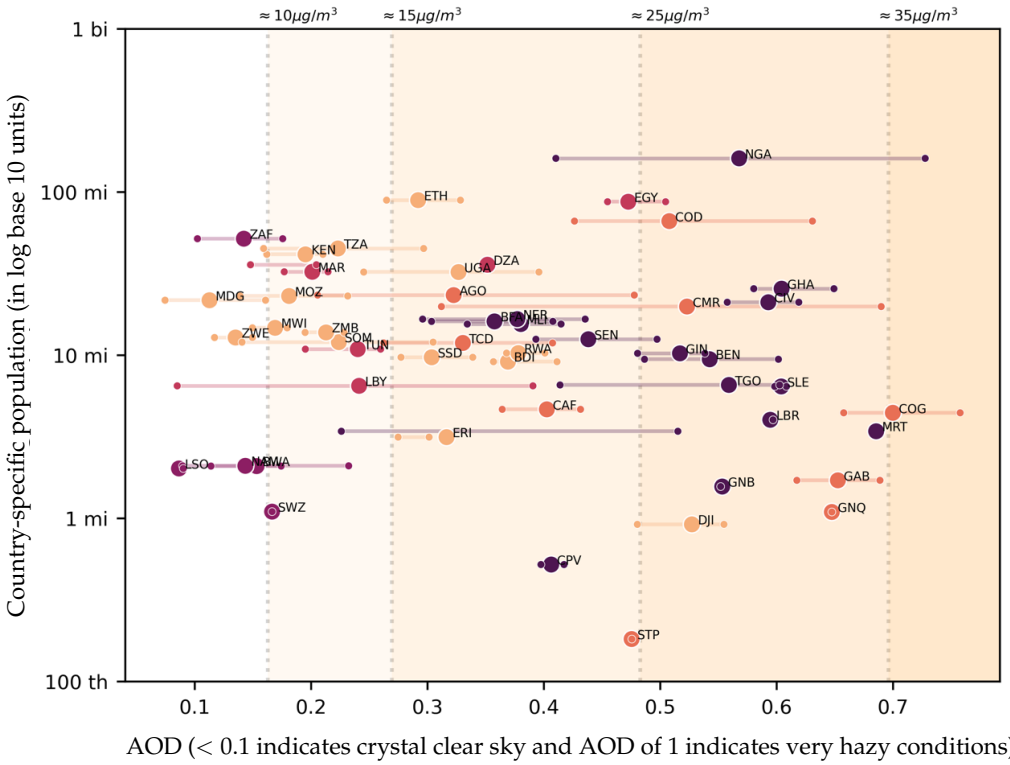

Notes: The panels present the African distribution of air pollution by aerosols as measured by Aerosol Optical Depth (AOD). We compute annual average AOD for each 1° cell. Panel (b) lines mark the 20th percentile, mean, and the 80th percentile of a country's AOD distribution, computed based on the distribution of AOD and population across cells corresponding to each country. In Panel (a), the y-axis shows cell population weighted density approximations. The x-axis in Panel (a) corresponds to levels of excess aerosol burden, a value of 0.5 (-0.5) indicates that a cell's AOD measure is 50 percent greater (smaller) than the global weighted mean. The x-axis in Panel (b) is in AOD units and tick-labels show AOD values. The vertical dashed lines corresponding to PM 2.5 thresholds in $\mu g/m^3$ units according to WHO interim targets (ITs). Background color corresponds to the IT ranges, with darker colors indicating lower air quality thresholds.

Figure 4: European population-weighted distribution of air pollution by aerosols, 2010

(a) 1° cell as the unit of observation (weighted by cell-population), by sub-regions

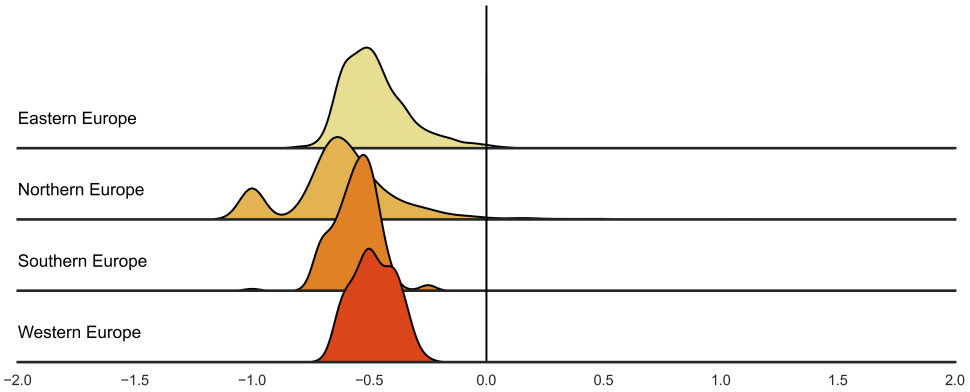

Excess aerosol burden relative to the global weighted mean

(b) Country-specific distributional ranges: P20 (*left-dot*), mean (*center-dot*), P80 (*right-dot*)

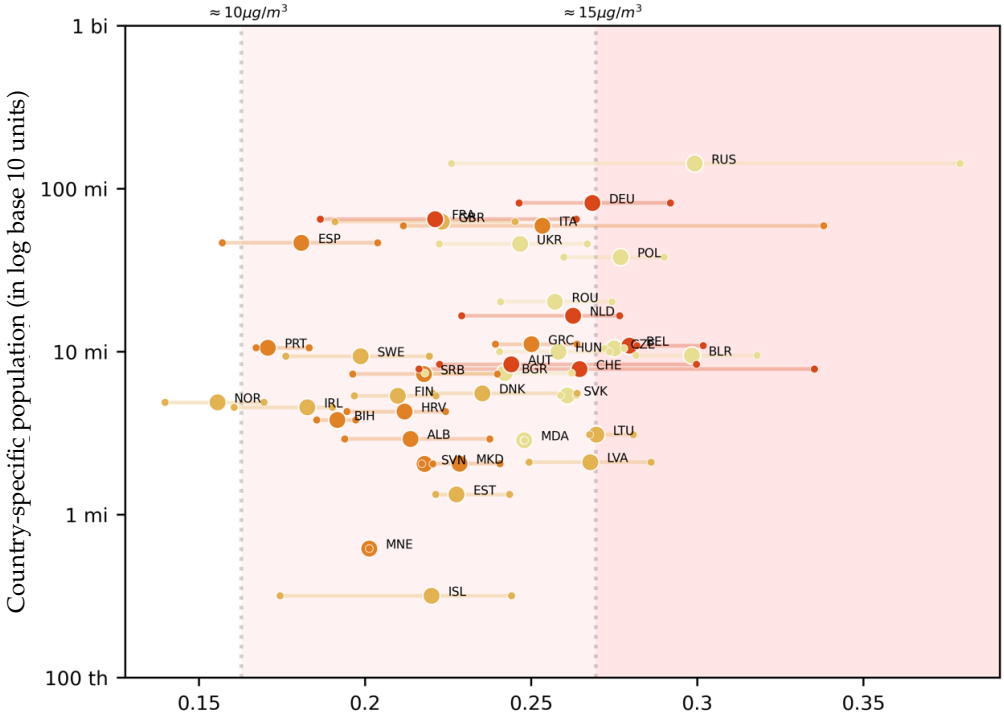

AOD (< 0.1 indicates crystal clear sky and AOD of 1 indicates very hazy conditions)

Notes: The panels present the European distribution of air pollution by aerosols as measured by Aerosol Optical Depth (AOD). We compute annual average AOD for each 1° cell. Panel (b) lines mark the 20th percentile, mean, and the 80th percentile of a country's AOD distribution, computed based on the distribution of AOD and population across cells corresponding to each country. In Panel (a), the y-axis shows cell population weighted density approximations. The x-axis in Panel (a) corresponds to levels of excess aerosol burden, a value of 0.5 (-0.5) indicates that a cell's AOD measure is 50 percent greater (smaller) than the global weighted mean. The x-axis in Panel (b) is in AOD units and tick-labels show AOD values. The vertical dashed lines corresponding to PM 2.5 thresholds in $\mu g/m^3$ units according to WHO interim targets (ITs). Background color corresponds to the IT ranges, with darker colors indicating lower air quality thresholds.

Figure 5: American population-weighted distribution of air pollution by aerosols, 2010

(a) 1° cell as the unit of observation (weighted by cell-population), by sub-regions

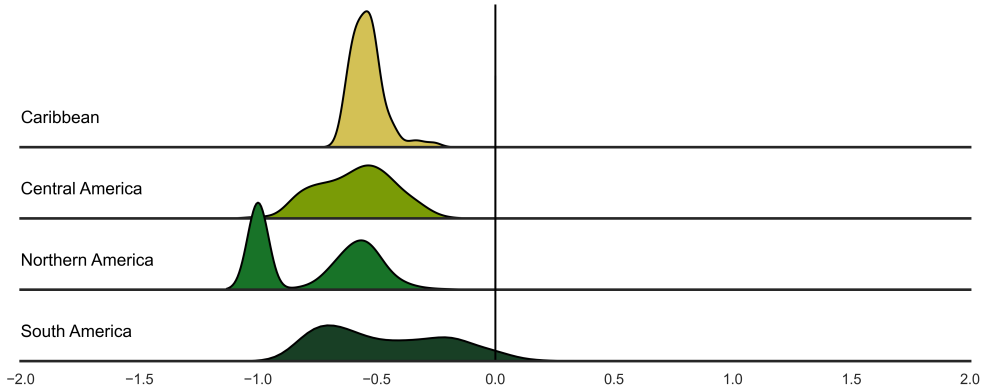

Excess aerosol burden relative to the global weighted mean

(b) Country-specific distributional ranges: P20 (*left-dot*), mean (*center-dot*), P80 (*right-dot*)

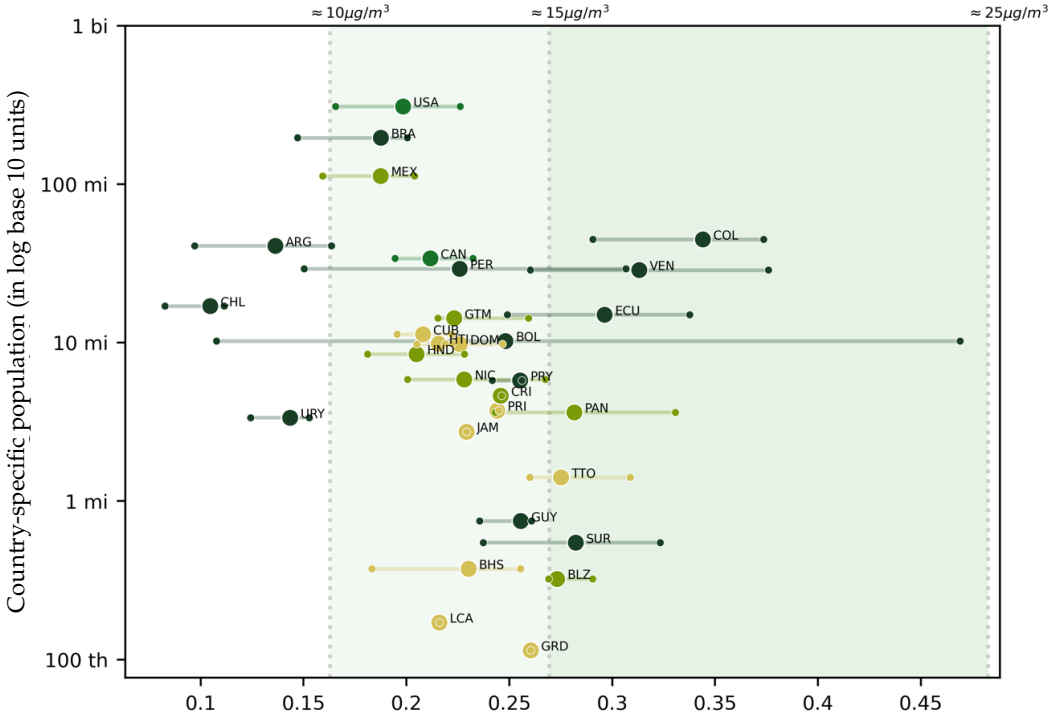

AOD (< 0.1 indicates crystal clear sky and AOD of 1 indicates very hazy conditions)

Notes: The panels present the American distribution of air pollution by aerosols as measured by Aerosol Optical Depth (AOD). We compute annual average AOD for each 1° cell. Panel (b) lines mark the 20th percentile, mean, and the 80th percentile of a country's AOD distribution, computed based on the distribution of AOD and population across cells corresponding to each country. In Panel (a), the y-axis shows cell population weighted density approximations. The x-axis in Panel (a) corresponds to levels of excess aerosol burden, a value of 0.5 (-0.5) indicates that a cell's AOD measure is 50 percent greater (smaller) than the global weighted mean. The x-axis in Panel (b) is in AOD units and tick-labels show AOD values. The vertical dashed lines corresponding to PM 2.5 thresholds in $\mu g/m^3$ units according to WHO interim targets (ITs). Background color corresponds to the IT ranges, with darker colors indicating lower air quality thresholds.

Figure 6: Oceanian population-weighted distribution of air pollution by aerosols, 2010

(a) 1° cell as the unit of observation (weighted by cell-population), by sub-regions

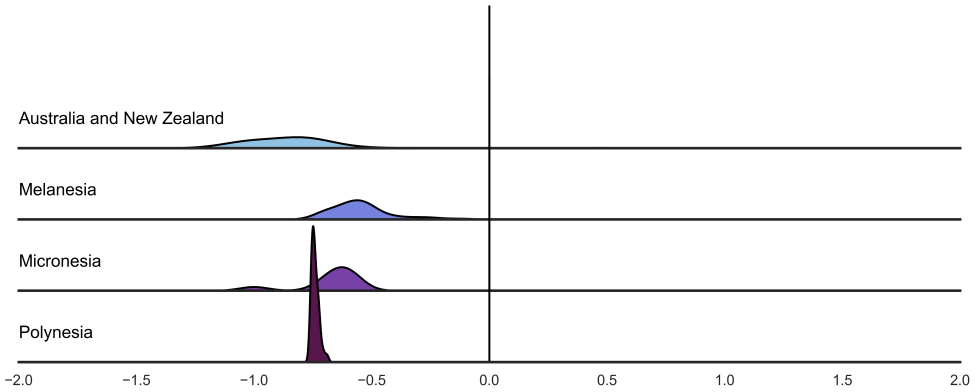

Excess aerosol burden relative to the global weighted mean

(b) Country-specific distributional ranges: P20 (*left-dot*), mean (*center-dot*), P80 (*right-dot*)

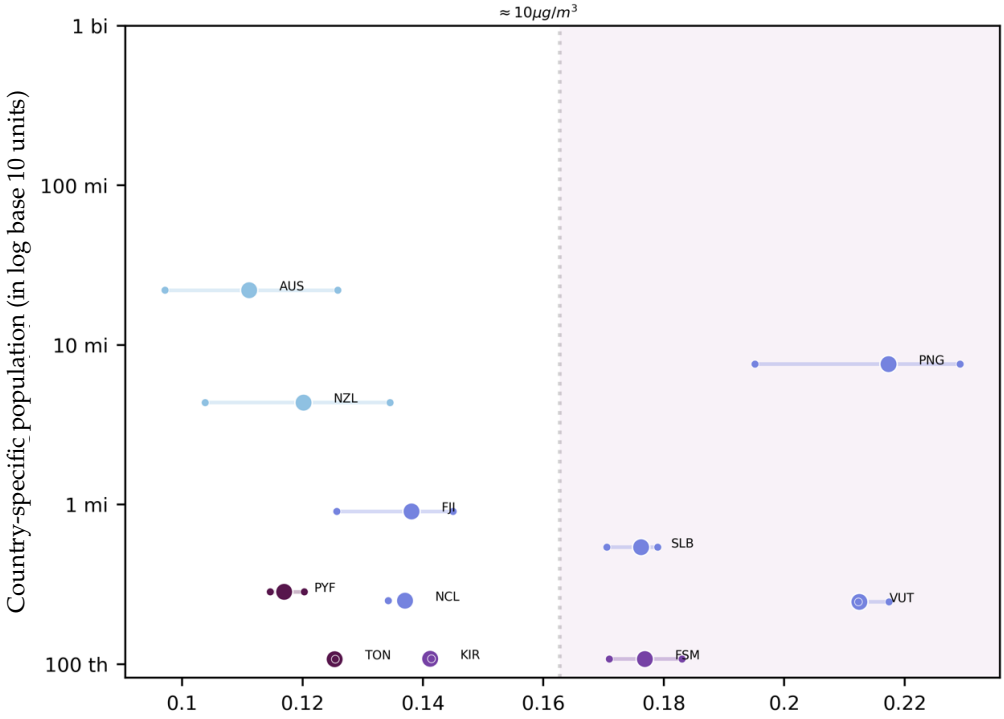

AOD (< 0.1 indicates crystal clear sky and AOD of 1 indicates very hazy conditions)

Notes: The panels present Oceanian distribution of air pollution by aerosols as measured by Aerosol Optical Depth (AOD). We compute annual average AOD for each 1° cell. Panel (b) lines mark the 20th percentile, mean, and the 80th percentile of a country's AOD distribution, computed based on the distribution of AOD and population across cells corresponding to each country. In Panel (a), the y-axis shows cell population weighted density approximations. The x-axis in Panel (a) corresponds to levels of excess aerosol burden, a value of 0.5 (-0.5) indicates that a cell's AOD measure is 50 percent greater (smaller) than the global weighted mean. The x-axis in Panel (b) is in AOD units and tick-labels show AOD values. The vertical dashed lines corresponding to PM 2.5 thresholds in $\mu g/m^3$ units according to WHO interim targets (ITs). Background color corresponds to the IT ranges, with darker colors indicating lower air quality thresholds.

Figure 7: Global association between air pollution by aerosols and GDP per capita, 2010

(a) National scatter plot, continental color groups, circle size represents relative population sizes

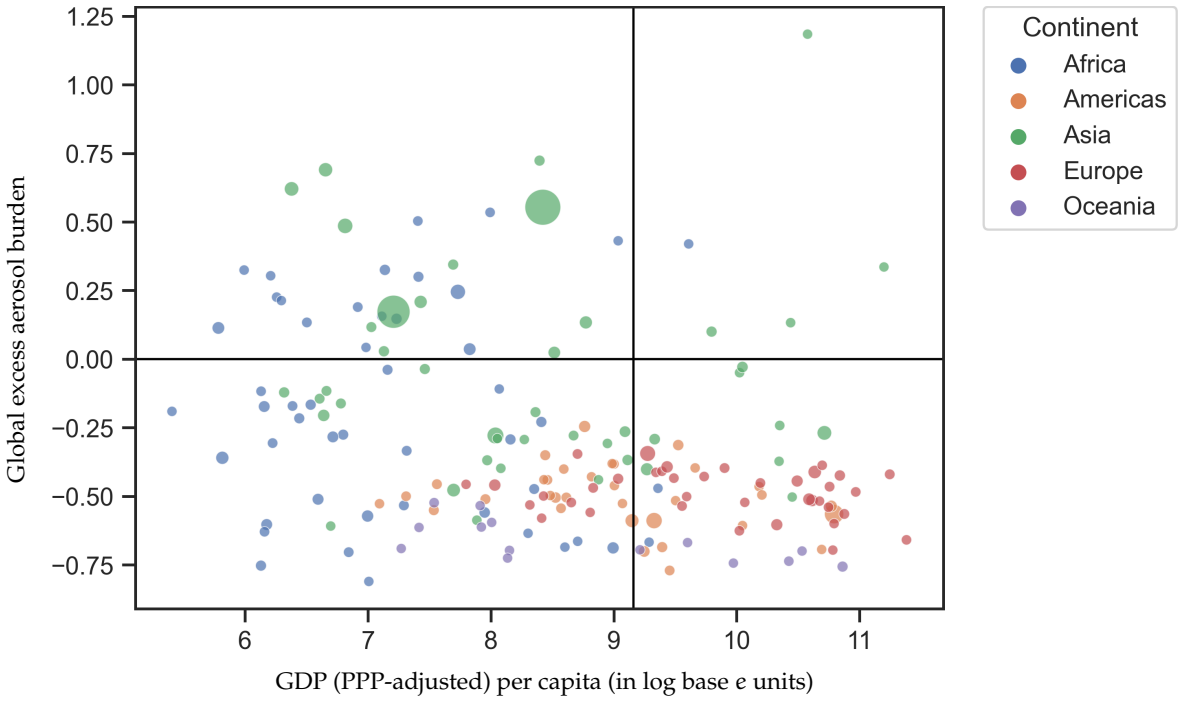

(b) National scatter plot, national population-weighted bivariate regression line

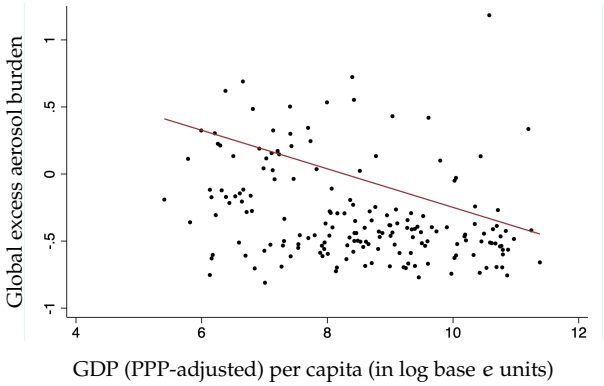

(c) Subnational scatter plot, subnational population weighted bivariate regression line

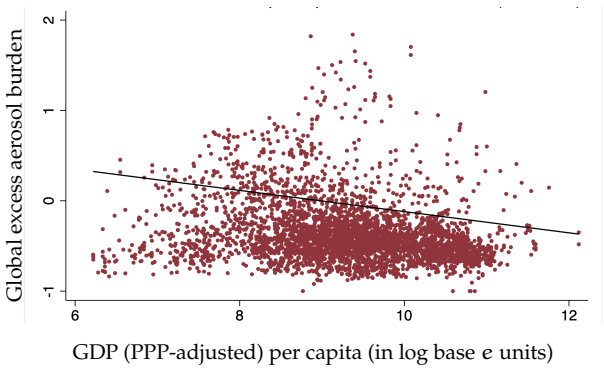

Notes: Panels (a) and (b) present national aggregates. Panel (c) presents subnational—first-level subnational administrative division—results. Across the panels, the x-axes correspond to levels of economic development as measured by GDP (Purchasing Price Parity adjusted) per capita in log base e units, and the y-axes correspond to relative exposures to air pollution by aerosols as measured by Aerosol Optical Depth (AOD). In Panel (a), colors distinguish countries by continental groupings, and the size of the scatter points are proportional to population sizes of each country. Additionally, in Panel (a), the black lines mark global weighted averages along each axis and divide countries into four quadrants for relative comparisons: upper-right, higher GDP per capita and AOD; upper-left, lower GDP per capita and higher AOD; bottom-left, lower GDP per capita and AOD; and bottom-right, higher GDP per capita and lower AOD. The y-axes across panels are in units of what we call global excess aerosol burden: A value of 0.5 (-0.5) indicates that a national or subnational unit's AOD measure is 50 percent greater (smaller) than the global weighted mean. We compute annual average AOD for each cell ($1° \times 1°$ longitude–latitude grid) and then generate national and subnational AOD as cell-population weighted averages. Subnational GDP and boundaries come from Kummu, Taka, and Guillaume (2018).

Table 1: Global association between air pollution by aerosols and GDP per capita, 2010

	Dependent variable: global excess aerosol burden					
	National regressions			Subnational regressions		
	(1)	(2)	(3)	(4)	(5)	(6)
(a): Common-slope global regressions						
GDP (PPP-adjusted) per capita (in log base e units)						
× Global	-0.075***	-0.144***	-0.037	-0.083***	-0.118***	-0.009
	(0.018)	(0.023)	(0.024)	(0.007)	(0.008)	(0.009)
R^2	0.09	0.19	0.57	0.04	0.05	0.37
Observations	178	178	178	3,902	3,712	3,709
Population weights	No	Yes	Yes	No	Yes	Yes
Continental fixed effects	No	No	Yes	No	No	Yes
(b): Continent-specific slope regressions						
GDP (PPP-adjusted) per capita (in log base e units)						
× Africa	-0.031	0.023	0.032	0.099***	0.052**	0.088***
	(0.053)	(0.054)	(0.060)	(0.027)	(0.020)	(0.023)
× Americas	-0.031	-0.027	-0.074*	-0.057***	-0.019***	-0.022***
	(0.021)	(0.018)	(0.041)	(0.011)	(0.005)	(0.008)
× Asia	-0.013	-0.053	-0.253***	-0.030	-0.026	-0.099***
	(0.044)	(0.054)	(0.045)	(0.022)	(0.021)	(0.022)
× Europe	-0.019	-0.037**	0.032	-0.055***	-0.016**	0.053***
	(0.014)	(0.014)	(0.020)	(0.006)	(0.006)	(0.008)
× Oceania	-0.040***	-0.065***	-0.064**	-0.061***	-0.071***	-0.077***
	(0.013)	(0.005)	(0.024)	(0.012)	(0.006)	(0.009)
Observations	178	178	178	3,902	3,712	3,709
Population weights	No	Yes	Yes	No	Yes	Yes
Continental fixed effects	Yes	Yes	Yes	Yes	Yes	Yes
Sub-continental fixed effects	No	No	Yes	No	No	Yes

Note: * $p < 0.1$; ** $p < 0.05$; *** $p < 0.01$. We regress global excess aerosol burden—which captures global relative exposures to air pollution by aerosols as measured by Aerosol Optical Depth (AOD)—on GDP (Purchasing Price Parity adjusted) per capita in log base e units. Results in Panel (a) present the global association, and results in Panel (b) allow for continent-specific associations. In columns (1)–(3), we use country-level data; in columns (4)–(6), we use subnational—first-level subnational administrative division—data. Results from columns (1) and (4) give equal weights to each national and subnational unit. Results from columns (2) and (5) use national or subnational population weights. In Panel (a), results from columns (3) and (6) control for continental fixed effects. In Panel (b), all columns allow for continent-specific slopes and intercepts, and columns (3) and (6) also control for sub-continental fixed effects for each sub-region shown in Panel (a) from Figures 3–4 (e.g., Northern Africa, East Asia, etc.). The dependent variable across regressions is in units of what we call global excess aerosol burden: A value of 0.5 (-0.5) indicates that a national or subnational unit's AOD measure is 50 percent greater (smaller) than the global weighted mean. We compute annual average AOD for each cell ($1^\circ \times 1^\circ$ longitude–latitude grid) and then generate national and subnational AOD as cell-population weighted averages. Subnational GDP and boundaries come from Kummu, Taka, and Guillaume (2018). See Figure 7 and Appendix Figure E.10 for scatter plots corresponding to panels (a) and (b).

ONLINE APPENDIX

Population burdens of air pollution around the world: Distributions, inequalities, and links to per capita GDP

Angelo Santos, Oscar Morales, Jere R. Behrman, Emily Hannum, Fan Wang

A Method

Population-weighted AOD distributions To analyze population-weighted air pollution by aerosol distributions, we define a discrete distribution of 2010 annual average AOD values over the set of all populated cells, where the cell-specific population mass is determined by GPWv4-based population estimates from around 2010. Specifically, let s_c be the share of global population in cell c, a_c be the average annual AOD at cell c, and C be the set of all gridded cells where $s_c > 0$. The global population-weighted annual average AOD distribution function, which provides the share of global population experiencing lower than a^* levels of annual average AOD, is equal to:

$$F(a^*) = P(a < a^*) = \sum_{c \in C} s_c \cdot \mathbf{1}\{a_c < a^*\} \ . \tag{8}$$

To compare aerosol distributions conditional on regional groupings based on supranational, national, and subnational boundaries, we define $C_r \subseteq C$ as the set of populated cells that intersect with the boundary enclosures of supranational, national, or subnational location r. For boundary data, we use national boundary data available in the GPWv4 population dataset (CIESIN Columbia University 2018), and the subnational boundary data embedded in the subnational GDP data from (Kummu, Taka, and Guillaume 2018). The share of population in cell c among population within location grouping r is $s_{c,r} = \frac{s_c}{(\sum_{\hat{c} \in C_r} s_{\hat{c}})}$, and the location-specific AOD distribution function is:

$$F_r(a^*) = P_r(a < a^*) = \sum_{c \in C_r} s_{c,r} \cdot \mathbf{1}\{a_c < a^*\} \ . \tag{9}$$

Given the location-specific distribution function, we compute mean exposure for each loca-

tion r:

$$\mu_r = \sum_{c \in C_r} s_{c,r} \cdot a_c \ . \tag{10}$$

The global weighted mean is $\mu_{\text{global}} = \sum_{c \in C} s_c \cdot a_c$. In our empirical analysis, we compute global, continental, regional, national, and subnational population weighted annual mean AOD exposures.

Given the discrete mass distribution over cells, the location-specific distribution function $F_r(a^*)$ is not invertible. Hence, we define the τ^{th} percentile of the location-specific distribution as the minimum a^* value where the share of population in location r with less than a^* level of annual average AOD is greater or equal to $\frac{\tau}{100}$, specifically:

$$\text{percentile}_r(\tau) = \min \left\{ a^* : F_r(a^*) \geqslant \frac{\tau}{100} \right\} \ . \tag{11}$$

Discussions in our empirical analysis focus on location-specific 20^{th} and 80^{th} as well as 10^{th} and 90^{th} percentiles, and use relative percentile ratios as a key measure for within location distributional variabilities.

Relative exposure and excess burden To measure relative exposures, we compute what we call excess aerosol burden: $e_{c,\hat{r}}$ is the excess aerosol burden of cell c with respect to location $\hat{r}$, and it measures the percentage deviation between cell-specific AOD value a_c and location-specific AOD value average $\mu_{\hat{r}}$:

$$e_{c,\hat{r}} = \frac{a_c - \mu_{\hat{r}}}{\mu_{\hat{r}}} = \frac{a_c}{\mu_{\hat{r}}} - 1 \ . \tag{12}$$

When $\hat{r}$ includes all global cells, we have $e_{c,\text{global}}$, the cell-specific global excess aerosol burden.

We also compute $e_{r,\hat{r}}$, which is the excess aerosol burden of location r with respect to location $\hat{r}$, where $\hat{r}$ (e.g., continent) encompasses r (e.g., countries within continent). Specifically, we compute the percentage deviation between the population-weighted mean exposure from location r and location $\hat{r}$:

$$e_{r,\hat{r}} = \frac{\mu_r - \mu_{\hat{r}}}{\mu_{\hat{r}}} = \frac{\mu_r}{\mu_{\hat{r}}} - 1 \ . \tag{13}$$

When r includes all cells within a country and $\hat{r}$ includes all global cells, $e_{\text{country,global}}$ provides

the country-specific excess aerosol burden relative to the global mean. If $e_{\text{country,global}} = 0$, a country's mean exposure level is the same as the global mean. A value of 0.5 or -0.5 for $e_{\text{country,global}} = 0$ indicates that a country's population-weighted AOD measure is 50 percent greater or smaller than the global population-weighted mean.

Importantly, excess aerosol burden also captures the percentage deviation between the share of ambient pollution that a population group is exposed to and the share of population they account for. Specifically, $e_{r,\hat{r}}$ can also be expressed as:

$$e_{r,\text{global}} = \frac{\overbrace{\left(\frac{\left(\sum_{c \in C_r} s_c\right) \cdot \mu_r}{\mu_{\text{global}}}\right)}^{\text{Location r global pop-weighted pollution share}}}{\underbrace{\left(\sum_{c \in C_r} s_c\right)}_{\text{Location r global population share}}} - 1 = \frac{\mu_r}{\mu_{\text{global}}} - 1 \, . \tag{14}$$

Because the term $\left(\sum_{c \in C_r} s_c\right) \cdot \mu_r$ appears in both the numerator and the denominator, it cancels out. A value of 0.5 or -0.5 for $e_{r,\text{global}}$ indicates that location r's share of global population-weighted air pollution is 50 percent greater or smaller than location r's share of global population.

AOD and $PM_{2.5}$ As a satellite-based measure of air pollution by aerosols, AOD measurements increase with greater concentrations of atmospheric particles, including $PM_{2.5}$ particles. While our analysis is focused on the distribution of air pollution by aerosols as measured by AOD, to assist with the interpretation of the magnitudes of AOD results, in the presentation and discussion of our AOD results, we match measured AOD values to approximate ranges of $PM_{2.5}$ values.

While AOD captures directly visibility experiences, the best-fitting model that maps between atmospheric aerosol measurements and on-the-ground ambient particulate matter exposure experienced by people is parameterized by heterogeneous topological and meteorological circumstances (Chu et al. 2016; Holben et al. 1998; Van Donkelaar et al. 2016; Yang et al. 2019). Overall, atmospheric-based AOD measures have been found to substantively and positively correlate with ground-based aerosol and $PM_{2.5}$ measurements (Bibi et al. 2015; Bright and Gueymard 2019; Chu et al. 2016), and AOD is often used as a predictor of ambient $PM_{2.5}$ exposures with locally and temporally calibrated prediction functions (Chen et al. 2022; Fu et al. 2018; Yang et al. 2019).

To create a globally consistent and transparent scale, we use a global linear model to relate our AOD estimates to existing global estimates of $PM_{2.5}$. Specifically, we relate the cell-specific annual average AOD values we derived to global gridded estimates of surface $PM_{2.5}$ concentration derived based on models that use satellite-based AOD measures as inputs and ground-based $PM_{2.5}$ data for calibration and model validation (Hammer et al. 2020). Regressing the $PM_{2.5}$ values from Hammer et al. (2020) on our AOD measures, we find that a bivariate linear model with subregion fixed effects provides a reasonable global fit with an R^2 of 0.78. We obtain similar fit and estimates when we restrict the data to only populated cells or when we use all available cells, and higher polynomial orders do not significantly improve the fit.

In our results discussions, we also compare the AOD-transformed $PM_{2.5}$ measures to the WHO interim targets for particulate matter air pollution.[A.1] These targets are used as guidelines for classifying the severity of $PM_{2.5}$ exposures. The WHO guideline recommends lowering annual average exposure levels to less than 35 $\mu g/m^3$, 25 $\mu g/m^3$, 15 $\mu g/m^3$, and 10 $\mu g/m^3$ as interim targets 1, 2, 3, and 4.

Within and across country distributions of air pollution by aerosols Combining global AOD measures and population data, we present in this section the overall population-weighted global distribution of air pollution by aerosols. In contrast to prior studies on global population-based inequality in ambient air pollution, which have focused on comparing means across regions and countries (Shaddick et al. 2018; Van Donkelaar et al. 2021; Van Donkelaar et al. 2016), we study global inequalities based by conducting comparisons within and across region as well as countries.

A.1. The report can be found here https://www.who.int/publications/i/item/9789240034228

B Data

B.1 AOD

AOD is a measurement of the size of particles present in the Earth's atmosphere, determined by their capacity to absorb and reflect light. This measurement depends on factors such as the composition, size, and concentration of the particles.

The NASA Aerosol Optical Depth (AOD) dataset is a publicly available collection of level-2 processed satellite images. Specifically, the AOD data is computed based on images collected by the TERRA satellite via MODIS instruments, and is accessible via NASA EarthData's Open-DAP protocol. (Cornillon, Gallagher, and Sgouros 2003; Xiong et al. 2020)

The AOD dataset has been continuously updated since 2002, with new satellite images regularly added. The satellite used to capture these images is TERRA, equipped with the MODIS (or Moderate Resolution Imaging Spectroradiometer) instrument, which provides a spatial resolution of 3km and a temporal resolution of 5 minutes. After capturing the images, a processing algorithm is used to extract information about the aerosol properties and produce the AOD measurement.

In our analysis, we collect AOD measurements for each 3km x 3km cell across the globe and aggregate them into 1-degree latitude and longitude combinations (~ 110km x 110km) . Figure E.1 illustrates the global availability of the AOD measures in 2010. This figure plots the frequency of AOD measures for 1-degree latitude-longitude combinations, showing that a considerable share of them are covered for more than a third of the year. However, some places where it is hard to process the satellite images do not have information, such as deserts and ice coverage.

The AOD measurement has been widely utilized in scientific research as a predictor of pollution, particularly in estimating the concentration of $PM_{2.5}$ particles (Chen et al. 2022; Fu et al. 2018; Yang et al. 2019). The correlation documented suggests that higher values of AOD are positively correlated with higher levels of $PM_{2.5}$, i.e. more air pollution. (Bibi et al. 2015; Bright and Gueymard 2019; Chu et al. 2016)

The availability of this global dataset allows us to conduct comprehensive analyses of air pollution exposure on a global scale, as well as the ability to focus on specific regions or areas of interest.

B.1.1 Data download

To Access the data, it is necessary to register a user and key in the Nasa EarthData website (Free registration) It allows one to create a connection with OpenDAP servers. OpenDAP is an extensively used cloud service used by dataset providers to store big datasets. In the case of NASA, creating an OpenDAP connection to make queries allows the user to access the AOD dataset at the finest level directly from your command prompt. This makes the process lighter as the user does not need to download the datasets to process them.

B.1.2 Aggregation over space along satellite track

Let AOD denote Let x and y index latitude and longitude respectively. $c = (x, y)$ is a vector of coordinates. Let t index time. Across time, NASA TERRA satellite, captures AOD data within a parallelogram with vertices $\{c_t^v\}_{v \in \{TL,TR,BL,BR\}}$.

As mentioned before, the satellite data information collected from NASA has finer data as 3kmx3km. However, to merge the pollution information with the SEDAC population dataset, we aggregated the cells into one-degree combinations. The aggregation was done using a ceiling round method, which rounded all the latitude and longitude information to 1 degree. For instance, if one location is identified by latitude 49.568 and longitude -34.543, the aggregation method will transform this geo-location into 49 (lat) and -34 (long). After rounding latitude and longitude columns, we took the average AOD associated with a particular latitude-longitude 1-degree combination.

In figure E.4 we plot the 1 degree x degree yearly measurements for 6 big cities in the world to illustrates how the cell annual average AOD is computed. On the x axis we have the days within the months, which are plotted on the y axis. For each combination of month-day we have either a missing (white cells) due to lack of observations in that particular day, or average AOD on that day (colorful cells). The cell average AOD is calculated by taking the mean of these values.

In figure E.4, we can also see that the NASA AOD measures capture higher concentrations of pollution in cities well known for their higher concentration of pollutants, as Beijing and New Delhi. Comparing these two cities with other cities plotted in E.4, we can see that the frequency of darker colors is higher across and within months compared to other locations.

B.2 The location X day file

Using OpenDap we could access all days of the year 2010 and construct a dataset that links locations and days. The first column will have the 1-degree combinations of latitude and longitude, where other columns correspond to the AOD measures of these locations on each day of the year. Using this location day information, we can create our measure of average AOD concentration in each cell in the world. The number of observations per cell depends on the ability of the algorithm to capture light, which is influenced by some factors such as clouds, desert, and ice. To deal with this problem, we use interpolation methods in our dataset.

B.2.1 Interpolation at time and location with missing information

The AOD dataset has global coverage but this coverage does not happen daily. Due to the satellite orbit, some cells are not going to be covered every day, which creates potential missing in the daily information. Another issue is the incapacity of the algorithm to process images from deserts, oceans, or ice due to refraction. This also creates potential missing values in the dataset. For example, the Sahara desert region does not have much information due to the impossibility of processing the image in desert conditions. Based on these issues, we can observe missings in two dimensions: time and location.

To test how sensitive our results are to these missing, we used interpolation methods to produce interpolated datasets based on the original AOD data. We used the Python package numpy (LINK) which contains implemented interpolation functions that can be applied to our dataset. Additionally, we perform interpolation using one dimension (location) and two dimensions (location, time).

Figure E.1 illustrates the global availability of the AOD measures in 2010. This figure plots the frequency of AOD measures for 1-degree latitude-longitude combinations, showing that a considerable share of them are covered for more than a third of the year. However, some places where it is hard to process the satellite images do not have information, such as deserts and ice coverage.

The figure shows the number of days in 2010 during which AOD data was available within each cell. The days are represented through shades of red from the darkest red (0 days) to the lightest red (all days in the year).

On days in which we do not have available AOD information for a particular cell, we use

information in neighboring locations and time periods to perform 3-dimensional—longitude, latitude, and time—interpolation and extrapolation to generate estimates for missing AOD data.

Given daily information, we compute annual average AOD exposures for each cell, first using only the raw data ignoring the days with missing values, and then separately using the raw data complemented with the interpolated and extrapolated estimates. Figure E.5 shows the distribution of our annual average AOD values at the cell level.

Due to the concentration of missing AOD data in regions with the least population, our population-weighted AOD distributional results based on the raw data and interpolated and extrapolated data are very similar. Our global inequality results presented in the text are based on annual averages of the raw data.

B.3 SEDAC Population file

SEDAC stands for Socioeconomic Data and Applications Center and is a center that relates earth science data to socioeconomic data. Specifically, in this analysis, we are exploiting the Gridded Population of the World version 4 (GPWv4) (CIESIN Columbia University 2018) which presents the estimates of the global population by gender and by age groups. These estimates come from the Population census or each country's population register. The data on the boundary comes from various sources including the GADM database of Global Administrative Areas, the Bureau of Statistics, the UN Office for the Coordination of Humanitarian Affairs, and the Center for International Earth Science Information Network (CIESIN) which hosts the SEDAC databases. Thus, the GPWv4 combines country-based administrative level data and administrative boundary data and distributes them into 30 arc-second grids (~ 1km at the equator) using a proportional allocation. The distribution by age and gender is done by using the proportion of males, females, and different age groups in each geographic unit and by applying those proportions to the 2010 estimates of the population in those same geographic units.

In our analysis, we used the 1-degree resolution (~ 110km) version of the data to create some input files for further analysis. We use the geographic information available to create unique geo-code IDs that will allow us to uniquely identify each grid. We used the population data available by groups and created different population groups by gender. It is good to be precise that the age groups are 5-years age groups and we have 14 different age groups ranging from

0-4 to 65-over. At the end, we get 28 different age $\times$ gender groups and then link those unique location IDs to the 28 different population groups.

Figure E.6 illustrates the global population distribution based on the SEDAC dataset in 2010, we plot the share of the world's population per cell. Some locations well known for their population sizes, such as India and China appear as hot spots in the heat map.

B.4 Subnational GDP data

The gridded global GDP dataset used in this paper is a product from the Gridded global datasets for Gross Domestic Product (Kummu, Taka, and Guillaume 2018). This data is derived from subnational GDP per capita data from Gennaioli et al. 2013, with the GDP per capita values adjusted for purchasing price parity and based on 2005 international dollars.

B.4.1 Source of data for GDP and Pop

For GDP per capita at the country level, we are using the World Bank's publicly available databases. This database has information on countries' GDP and is linked with the ISOCODE and ISONAMES for each country. Using these codes, we can merge the GDP and the pollution measures by using our key location files, which are all linked through the 1-degree geolocation combinations.

To get the country population info, we aggregated all the cell information within a country to get its population estimation using SEDAC. However, this method may have been issued due to the size of the cells, which led us to use other population data sources as robustness.

B.5 Merging and National and subnational boundaries

We combine the 2010 annual average AOD across 1° cell with the cell-specific total population estimates from around 2010. Because cells without any population will not impact population weighted statistics, we select the subset of of cells from the annual average AOD vector which has corresponding non-zero cell-specific population estimates. Additionally, to allow for the comparisons of population-weighted AOD distributions across and within countries and economies, we identify the subset of populated-cells that intersect with national-level boundary enclosures. To consider the relationship between population-weighted AOD distribution and GDP per capita at the subnational level, we also identify subsets of populated-cells

that interesect with subnational boundary data embedded in the subnational GDP data from (Kummu, Taka, and Guillaume 2018).

B.5.1 Country Boundaries

To identify which country is associated with the 1-degree latitude longitude combinations, we use SEDAC as the input data. The raster from SEDAC has two layers that inform the country in a particular degree combination. First, they inform the ISOCODE, an international standardized code for each country. Two, they also inform the international standardized acronyms for these countries. For example, Brazil's ISOCODE is 076 and its acronym is BRA. With this, we can create our country key file linking degree combinations and country information, as region and subregion. The input data used by SEDAC to categorize these boundaries are the censuses.

The fact that we are using 1-degree latitude longitude combinations can lead to imprecise borders due the the size of the cells. 1 degree corresponds to approximately 111 km, which can incorporates full cities. For example, figure E.3 shows how the cells are allocated to different countries in the world. We can see that the size of cell makes the allocation of some land to countries that it is not actually precise. For example, NASA's categorize part of Peru, Bolivia, Paraguay, and Uruguay to Brazil. This can impact the measurements if this include major cities or populated areas. An specific case is Santiago in Chile, which is allocated to Argentina due the size of the cells. Because of this, a important part of Chile that concentrates 40 % of its population and the most polluted region is allocated to Argentina. This can impact the inequality and mean measures of countries depending on its size and shape.

B.5.2 How do we use it, matching of coordinates to boundaries

To match these coordinates we created a file called skeleton, which includes all the 1-degree combinations in the world. Using SEDAC, we can build a dataset with three columns, latitude and longitude combination (one degree), ISOCODE, and ISONAME. After merging these files, we can use it to merge with our population data also linked using the latitude-longitude combinations.

C Integrating Climatic and Population Data

C.1 Program and Framework for analysis

The key file inputs make possible the merge between the geocoded pollution, population, and country datasets. In our analysis, we used two file inputs:

1. key_loc.csv

2. key_country_code_finer_subregions.csv.

The first key file has an id for every latitude-longitude combination at 1 degree level. The IDs were constructed using the following pattern. The latitude and longitude numbers were transformed into strings and concatenated (using "_" to separate the numbers) into one string called "geo_id ". For example, the location defined by latitude 45 and longitude -67 has the geo_id as "45_-67". After constructing all the possible geo_ids combinations, we sorted the location by latitude and longitude and assigned a number to each geo_id following the ascending order. This new column is called id_location and it is used to merge locations across different datasets, such as the pollution and the population geocoded information.

The second key file has the id_location and geo_id columns associated with geographical locations in the world. four layers of location: continent, subregion, and country. For instance, we know what are the latitude and longitude combinations that are associated with specific continents, sub-regions, and countries, which makes it possible to merge geocoded information from other datasets.

D Additional Results on heat exposure for children

D.1 Overall global distribution

D.1.1 Global country-level distribution

Figure E.7 presents histograms for the global relative distribution of air pollution by aerosols as measured by Aerosol Optical Depth (AOD). The x-axis is in units of global excess aerosol burdens. We compute annual average AOD for each $1^\circ \times 1^\circ$ longitude–latitude grid (cell) and generate country-specific AOD measures as cell-population weighted averages. The country-based distribution in Panel (a) uses country-specific AOD, weighted by aggregate population estimates for each country. The cell-based distribution in Panel (b) uses cell-specific AOD, weighted by cell-specific population estimates. The population weights are important because distributions where national or subnational units have equal weights mask the heterogeneous population burdens of exposure across geographical units.[D.1]

The variance for the cell-based distribution of in Panel (b) is 1.7 times larger than the country-based distribution in Panel (a), illustrating the wider distribution at the cell level. Additionally, Panel (a)'s country-level distribution of global excess aerosol burden ranges from -0.81 to 1.18, and has an 80^{th} percentile that is 1.44 times larger relative to its 20^{th} percentile. In contrast, Panel (b)'s cell level distribution of global excess aerosol burden ranges from approximately -1.0 to 10.06, and has an 80^{th} percentile that is 3.62 times more exposed than the 20^{th} percentile.

Comparisons between the Panels demonstrate that country-level information masks the inequalities across cells within countries. Our analysis in the following sections focus on population-weighted cell-based distributions.

D.1.2 Global cell-level distribution

Panel (a) of Figure 1 presents a global map of the relative distribution of air pollution by aerosols - calculated according to equation (**??**) - matching cell-specific AOD to cell locations. The colors correspond to levels of global excess aerosol burdens—darker shades of green (red) represent greater magnitudes of negative (positive) excess burdens.

D.1. In Appendix Figure E.7, we present un-weighted histograms. Comparing the distributions with and without weights, we can see a shift of the weighted distributions to the right. These shifts highlight the importance of considering the population weights, as our interest is how individuals in countries are exposed to air pollution.

The map shows that Asia and Africa have relatively higher levels of air pollution by aerosols. Focusing on countries, India, China, and Pakistan stand out as large countries with areas experiencing high levels of excess aerosol burdens. In contrast, Australia, Mexico, and Argentina are also large economies but have relatively lower levels of excess aerosol burdens. Additionally, there are variations in the within-country heterogeneities of exposures. For example, locations in the southeastern and northwestern regions of China have high excess burdens, but areas in northern and southwestern China have relatively lower levels of excess burdens. In contrast, countries within Western Europe and North America tend to have limited variations concentrated around lower levels of excess burdens.

D.2 Regional distribution

D.2.1 Africa

The most populous African country, Nigeria, has an annual average AOD of 0.56 ($\approx 28.98\,\mu g/m^3$ of $PM_{2.5}$), which is behind WHO interim target 2. Nigeria's average exposure level corresponds to a global excess aerosol burden of 0.24, meaning that Nigeria's global share of air pollution by aerosols is 24% larger than its population share. Exposure inequalities are significant within Nigeria—Nigerian population at the 80^{th} (90^{th}) percentile of aerosol distribution are 77% (106%) more exposed than those at the 20^{th} (10^{th}) percentile. One of the least populous countries in Africa, Sao Tome and Principe, has an average annual AOD of 0.47 ($\approx 24.65\,\mu g/m^3$ of $PM_{2.5}$), just passing WHO interim target 2. In contrast to Nigeria, relative population exposure percentiles are close to 1 due to the small size of the country.

D.2.2 Americas

South America has the highest average annual AOD at 0.22 ($\approx 12.93\,\mu g/m^3$ of $PM_{2.5}$). Central America has the lowest average annual AOD at 0.19 ($\approx 11.65\,\mu g/m^3$ of $PM_{2.5}$). All regions in the Americas, on average, have reached WHO interim targets 3.

The most populous country in the Americas, the United States of America, has an annual average AOD of 0.19 ($\approx 11.67\,\mu g/m^3$ of $PM_{2.5}$), close to reach WHO interim target 4. The US's average exposure level corresponds to a global excess aerosol burden of -0.56, meaning that the US's global share of air pollution by aerosols is 56% smaller than its population share. Exposure inequalities are important but limited in the US—Americans population at the 80^{th}

(90^{th}) percentile of aerosol distribution are 36% (71%) more exposed than those at the 20^{th} (10^{th}) percentile. One of the least populous countries in the Americas, Saint Lucia, has an average annual AOD of 0.21 ($\approx$ 12.49 $\mu g/m^3$ of $PM_{2.5}$). Relative population exposure percentiles is equal to 1 in Saint Lucia. Not all countries with low population have no within-country exposure variabilities. Suriname, which is another low population country in the Americas, has a similar AOD level as Saint Lucia, but greater within-country variabilities—Surinamese population at the 20^{th} percentile of aerosol distribution are 36% more exposed than those at the 80^{th} percentile.

D.2.3 Asia

The most populous Asian country, China, has an annual average AOD of 0.7 ($\approx$ 35.58 $\mu g/m^3$ of $PM_{2.5}$), which is behind WHO interim target 1, indicating very hazardous levels of average air pollution by aerosols. China's average exposure level corresponds to a global excess aerosol burden of 0.55, meaning that China's global share of air pollution by aerosols is 55% larger than its population share. Exposure inequalities are large within China— the Chinese population at the 80^{th} (90^{th}) percentile of aerosol distribution are 111% (216%) more exposed than those at the 20^{th} (10^{th}) percentile. One of the least populous countries in Asia, Qatar, has an average annual AOD of 0.60, which is similar to the level in China. Relative population exposure percentiles are equal to 1 due to the geographical confines of Qatar.

D.2.4 Europe

The most populous European country, Russia, has an annual average AOD of 0.29 ($\approx$ 16.39 $\mu g/m^3$ of $PM_{2.5}$), which is behind WHO interim target 3. Russia's average exposure level corresponds to a global excess aerosol burden of -0.34, meaning that Russia's global share of air pollution by aerosols is 34% smaller than its population share. Exposure inequalities are significant within Russia—Russian population at the 80^{th} (90^{th}) percentile of aerosol distribution are 67% (130%) more exposed than those at the 20^{th} (10^{th}) percentile. One of the least populous countries in Europe, Iceland, has an average annual AOD of 0.21 ($\approx$ 12.68 $\mu g/m^3$ of $PM_{2.5}$), close to reaching WHO interim target 4. Despite its limited population, there are exposure variabilities in Iceland due to its large geography—Icelandic population at the 80^{th} (90^{th}) percentile of aerosol distribution are 39% (49%) more exposed than those at the 20^{th} (10^{th}) percentile.

D.2.5 Oceania

Australia is the most populated country in the Oceania region and the least populated is Palau. In AOD terms, the mean exposure to pollution in Australia is 0.11, whereas the inequality measured using the ratio between 80^{th} and the 20^{th} percentiles indicates 29% more exposure to pollution to the upper side of the distribution. If we consider the extremes percentiles ratios, the 90^{th} percentile is 48% more exposed to pollution in comparison to the 10^{th} percentile. For Palau, the mean AOD exposure is 0.13, whereas the inequality using the percentile ratios in 1.03 and 1.03 for both ratios, indicates 3% more exposure faced by the upper part of the distribution. In $PM_{2.5}$ terms, the mean exposure faced by Australia is 21.23, higher than the third worse level recommendation by WHO, and the inequality measure for the 80^{th} measure is 19% and 30% for the 90^{th} percentile ratio. For Palau, the pm is 2.5. measures imply a mean exposure of 8.89 (below WHO guidelines) and the ratio for both inequality measures is 1.02, i.e., 2% more exposure faced by the upper part of the population distribution.

E Additional Figures and Tables

Figure E.1: Number of days with AOD data available for each 1° × 1° longitude–latitude grid, 2010

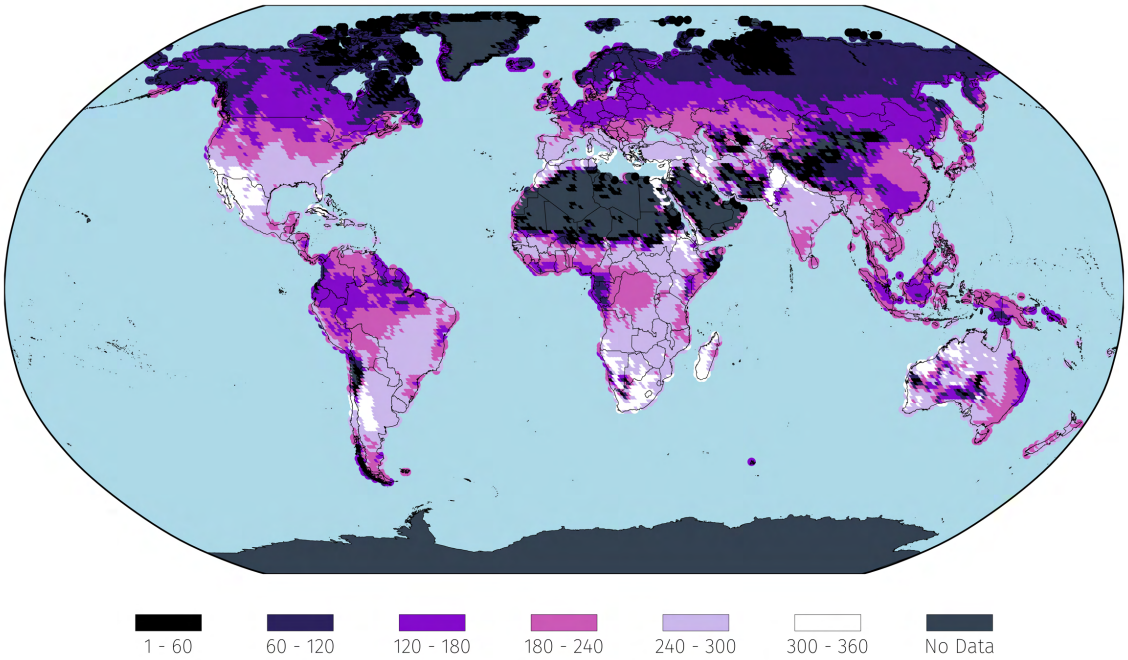

Notes: The figure presents the geographical and temporal availability of Aerosol Optical Depth (AOD) data, our global proxy for ambient particulate matter pollution exposures. For our analysis, we download raw AOD data available at 3km × 3km resolution and compute average daily AOD on each day of the year with available AOD measurements for each 1° × 1° longitude–latitude grid (cell). The figure shows the number of days in 2010 during which AOD data was available within each cell. The days are represented through shades of purple and pink from the darkest purple (1 day) to the lightest pink (almost all days in the year); days with zero data are represented by a gray color. Due to the concentration of missing AOD data in regions with the least population, our population-weighted AOD distributional results based on the raw data and interpolated and extrapolated data are very similar. Our global inequality results presented in the text are based on annual averages of the raw data.

Figure E.2: Population shares in areas with no raw AOD measurements 1° × 1° longitude–latitude grid, 2010

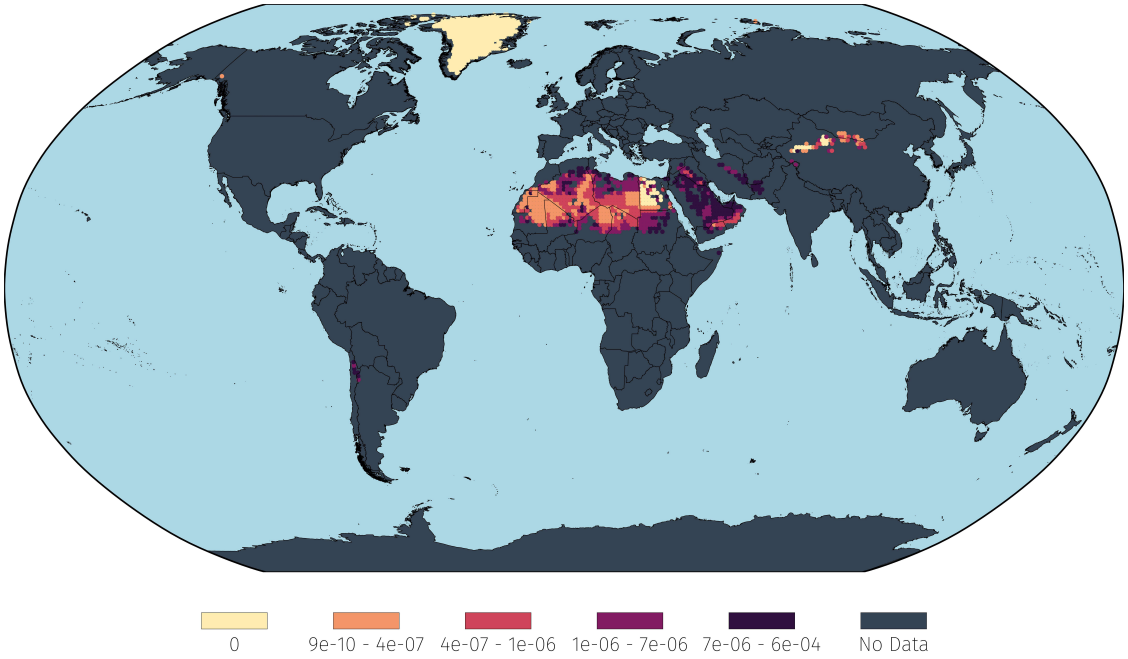

Notes: The figure plots the population shares of areas for which no AOD measurements exist. The share of global population represented by all colored areas amounts to just 0.00602 with 99.8% of cells in this section having a population share below the mean population share (0.000128) in areas with existing AOD measurements. Similarly, 85.8% of cells in this area have values below the median population measure (0.0000069) in areas for which AOD values exist. This means that above-global-average AOD measurements would have to had existed in these areas for our global population-weighted AOD mean to remain the same, otherwise our global mean would be lower than what was calculated meaning relative burden measures can be considered conservative estimates.

Figure E.3: $1° \times 1°$ longitude–latitude grids over select countries

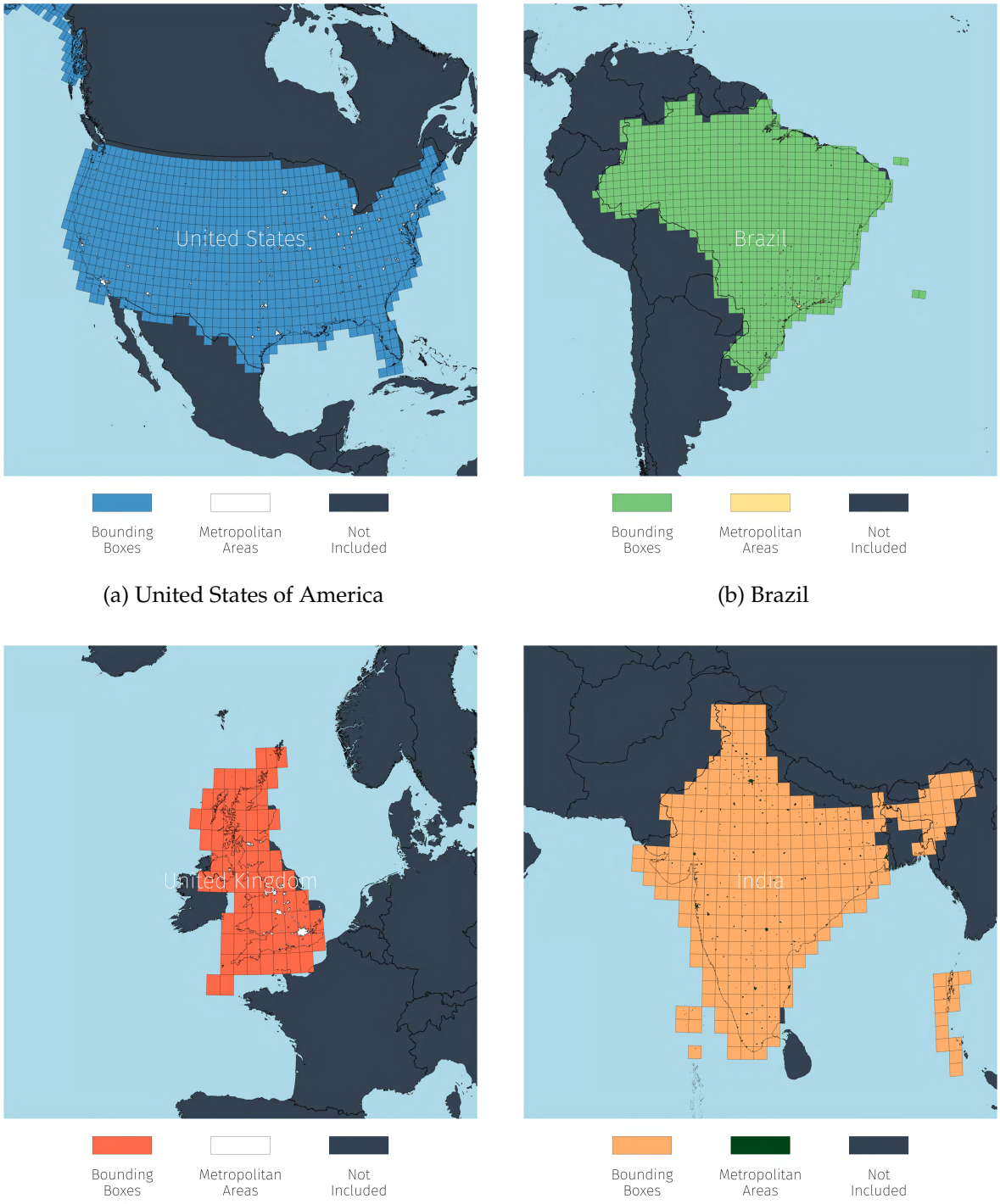

(a) United States of America

(b) Brazil

(c) United Kingdom

(d) India

Notes: We include plots displaying $1^o \times 1^o$ boxes corresponding to the area represented by a given $1^o \times 1^o$ coordinate point, over select countries along a spherical surface. These boxes serve as a visual illustration of the area along which we aggregate our AOD data for a given day; the average AOD in a given $1^o \times 1^o$ area for a given day is then associated to the new $1^o \times 1^o$ coordinate point. The classification of a given coordinate as belonging to a given country was determined by NASA's SEDAC. Our next figure illustrates several of these daily figures for $1^o \times 1^o$ areas corresponding to select major cities across the world. To arrive at the final AOD measurement we use in our analysis, we average these daily values to arrive at an annualized figure.

Figure E.4: AOD measurement heatmaps for major cities by $1° \times 1°$ longitude–latitude grids, 2010

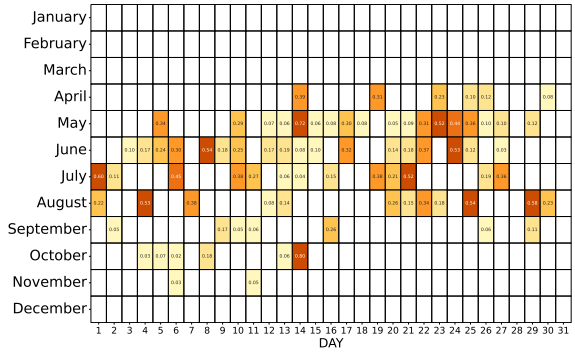

(a) New York City, United States

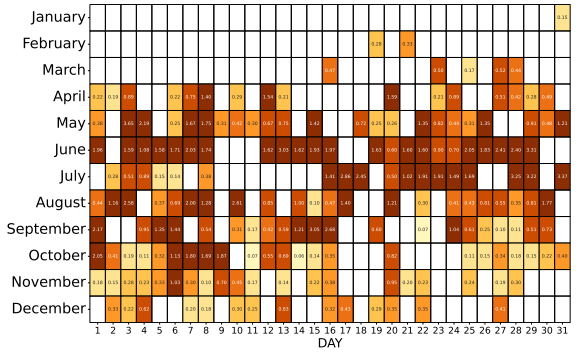

(b) Beijing, China

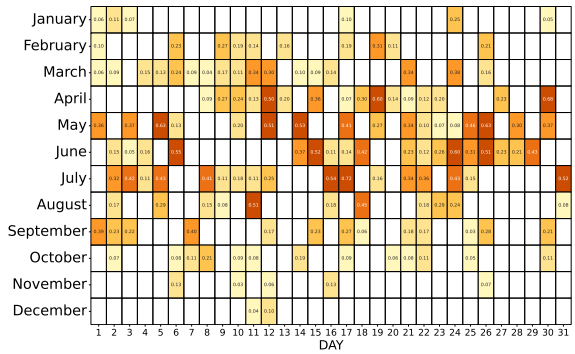

(c) London, United Kingdom

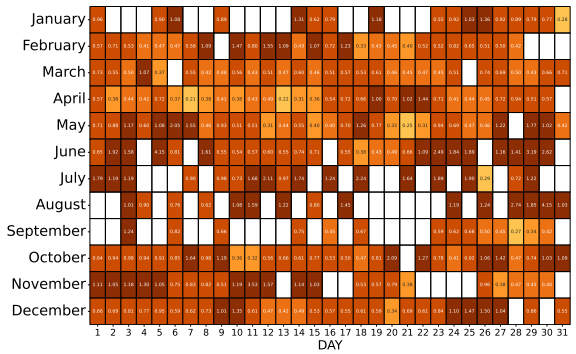

(d) New Dehli, India

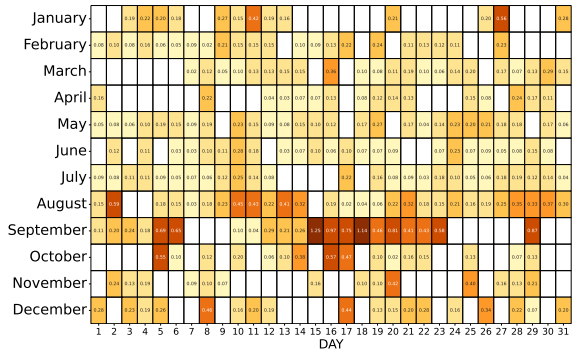

(e) São Paulo, Brazil

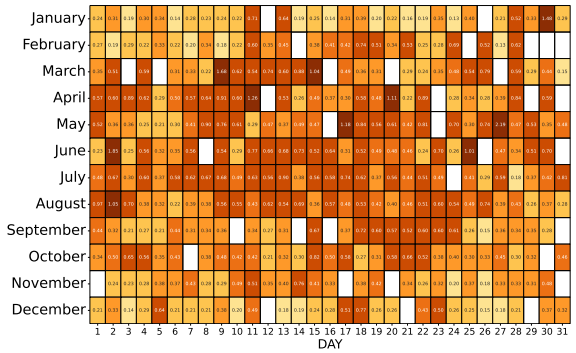

(f) Cairo, Egypt

Notes: We include AOD measurements captured on given days over the year 2010 over single $1^o \times 1^o$ grids that capture all or the majority of the area covered by major global cities as an illustration of the measurements that are used to compute annual averages over a given coordinate point.Cells are colored along the same scale with darker colors indicating higher AOD values and empty cells indicating that no data was able to be collected for that day. The coordinate grid that represents a city was chosen by applying the ceiling function to the longitude and latitude values of a city's central coordinates. These chosen cities are visible in the previous figure within their respective country.

Figure E.5: Daily-averaged-then-annualized AOD values for each 1° × 1° longitude–latitude grid, 2010

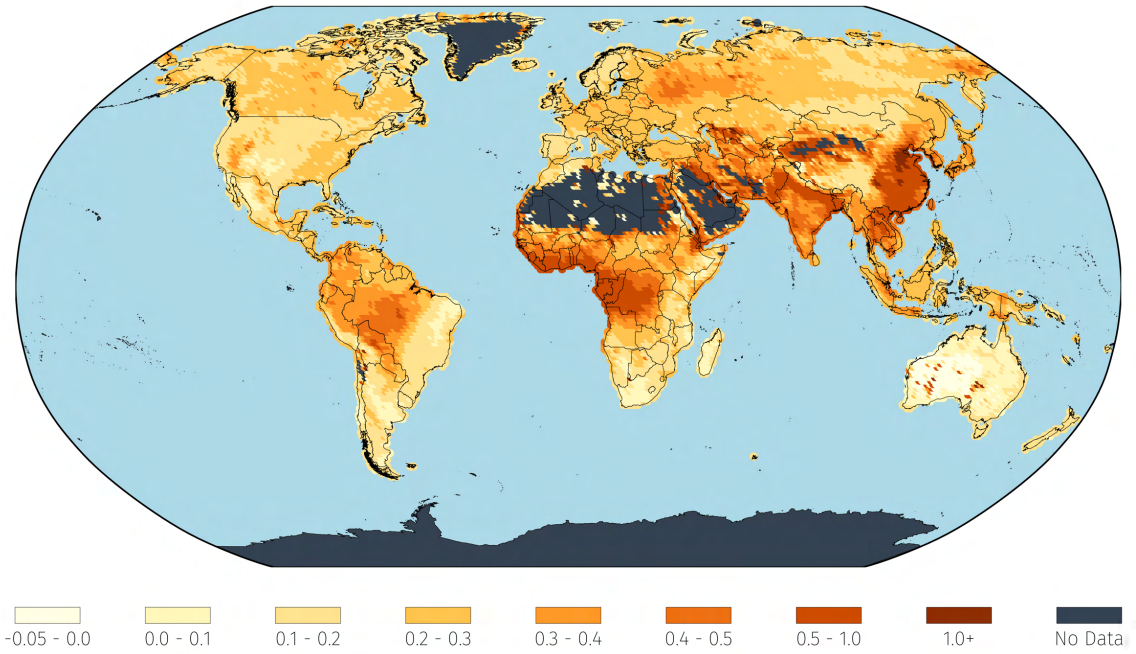

Notes: The figure presents the Aerosol Optical Depth (AOD) values for each coordinate grid, globally, as computed by first averaging collected values in a given day for a given coordinate, for each day, then annualized across daily data, for 2010. Darker shades of orange indicate higher levels of AOD

Figure E.6: GPWv4 population shares for each 1° × 1° longitude–latitude grid, 2010

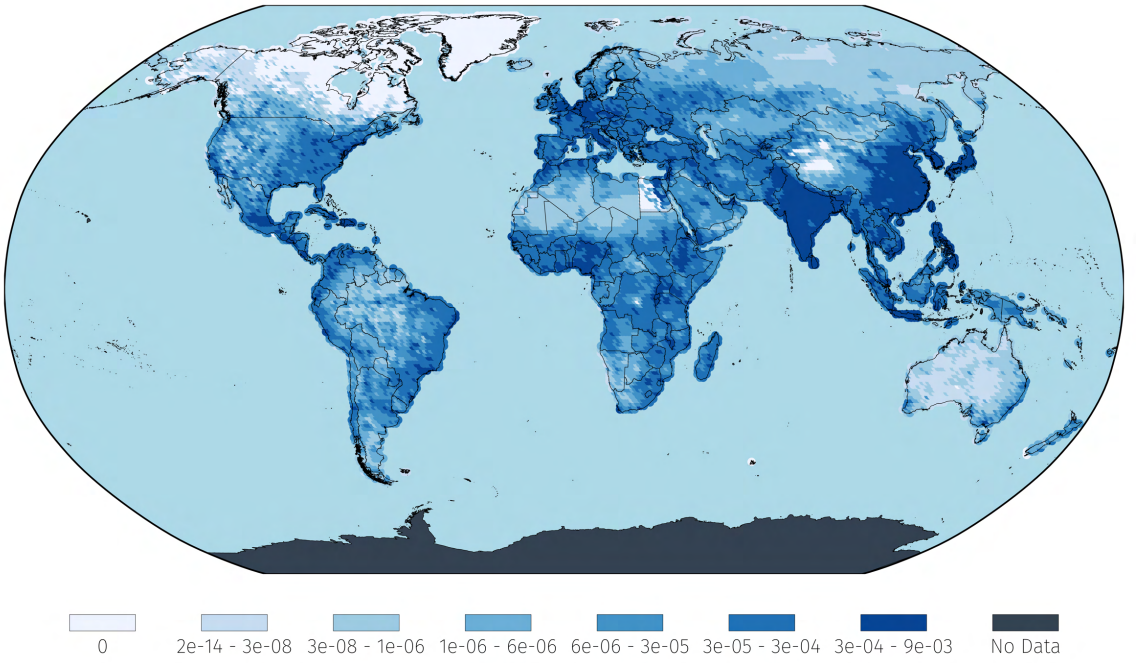

Notes: The figure presents raw population figures as part of SEDAC's GPWv4 population data collection, for 2010. The units of measurements are cell-level global population shares for every 1° × 1° grid. Darker shades of blue indicate a higher population share.

Figure E.7: Global dispersion of air pollution by aerosols, 2010

(a) Country as the unit of observation (equal weight for each country)

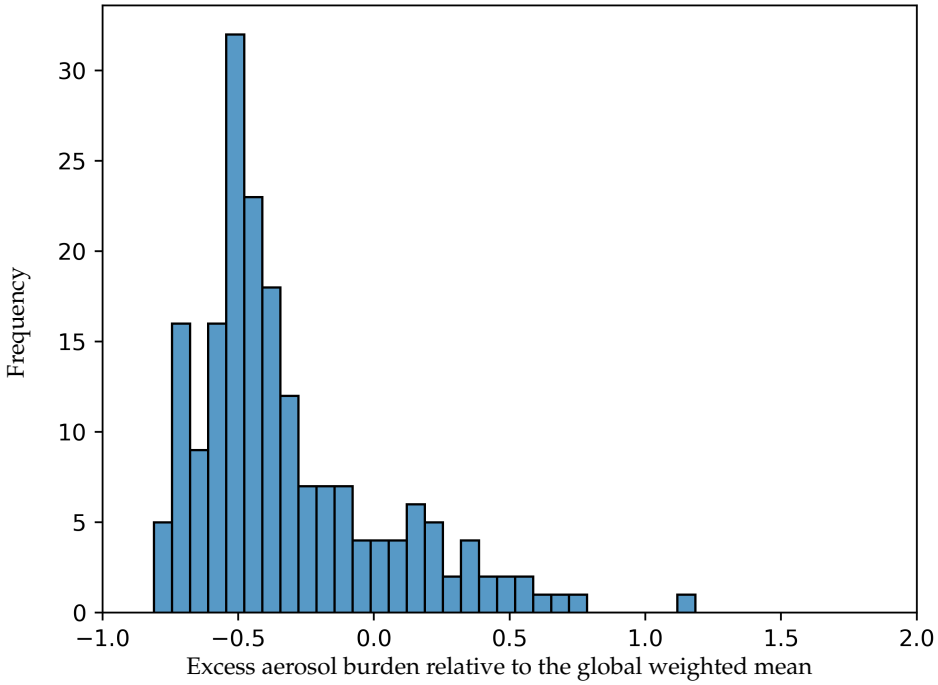

(b) 1° cell as the unit of observation (equal weight for each cell)

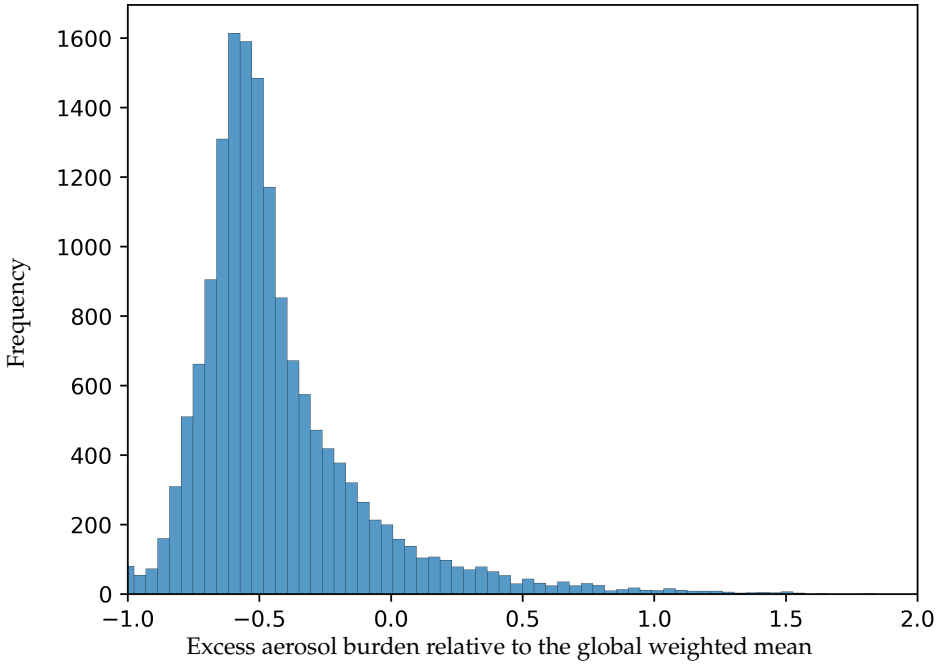

Notes: The panels present the global relative dispersion of air pollution by aerosols as measured by Aerosol Optical Depth (AOD). We compute annual average AOD for each cell ($1° \times 1°$ longitude–latitude grid) and then generate country-specific AOD as cell-population weighted averages. In contrast to Figure **??**, Panel (a) and (b) here treat each country or cell as a unit of observation with equal weights. The y-axis shows frequencies, counting the number of countries or cells. The x-axis is in units of what we call global excess aerosol burden: A value of 0.5 (-0.5) indicates that a country or cell's AOD measure is 50 percent greater (smaller) than the global weighted mean.

Figure E.8: Continental dispersion of air pollution by aerosols, 2010

(a) Country as the unit of observation (weighted by country-population), by continents

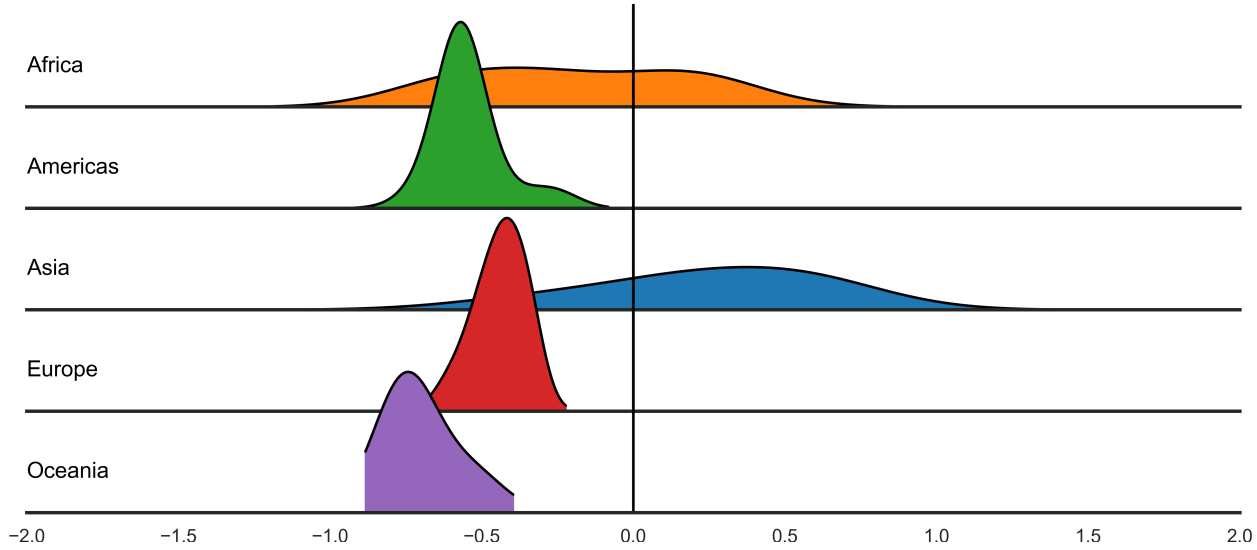

(b) Country as the unit of observation map

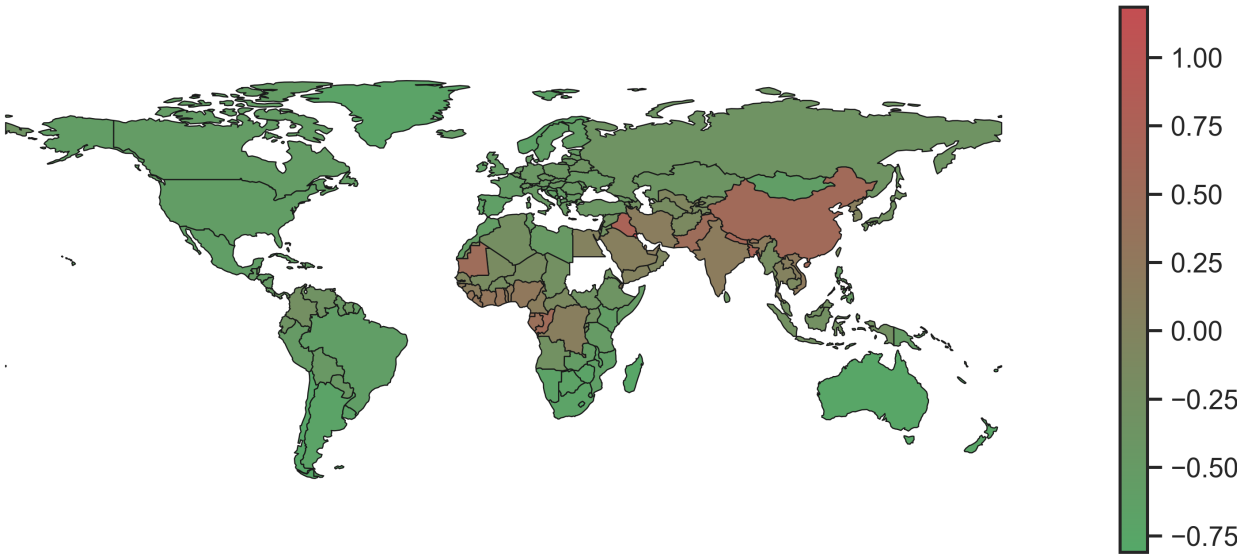

Notes: The panels present the global relative dispersion of air pollution by aerosols as measured by Aerosol Optical Depth (AOD). We compute annual average AOD for each cell ($1° \times 1°$ longitude–latitude grid) and then generate country-specific AOD as cell-population weighted averages. In contrast to Figure 1, Panel (a) treats each country as the unit of observation, weighted by aggregate population estimates for each country, and Panel (b) matches country-specific AOD to country locations. In Panel (a), the y-axis shows country population weighted density approximations. The x-axis in Panel (a) and colors in Panel (b) correspond to what we call global excess aerosol burden: A value of 0.5 (-0.5) indicates that a country's AOD measure is 50 percent greater (smaller) than the global weighted mean. In Panel (b), darker shades of green (red) correspond to greater magnitudes of negative (positive) excess burdens.

Figure E.9: Continental dispersion of air pollution by aerosols, relative to continent-specific weighted means, 2010

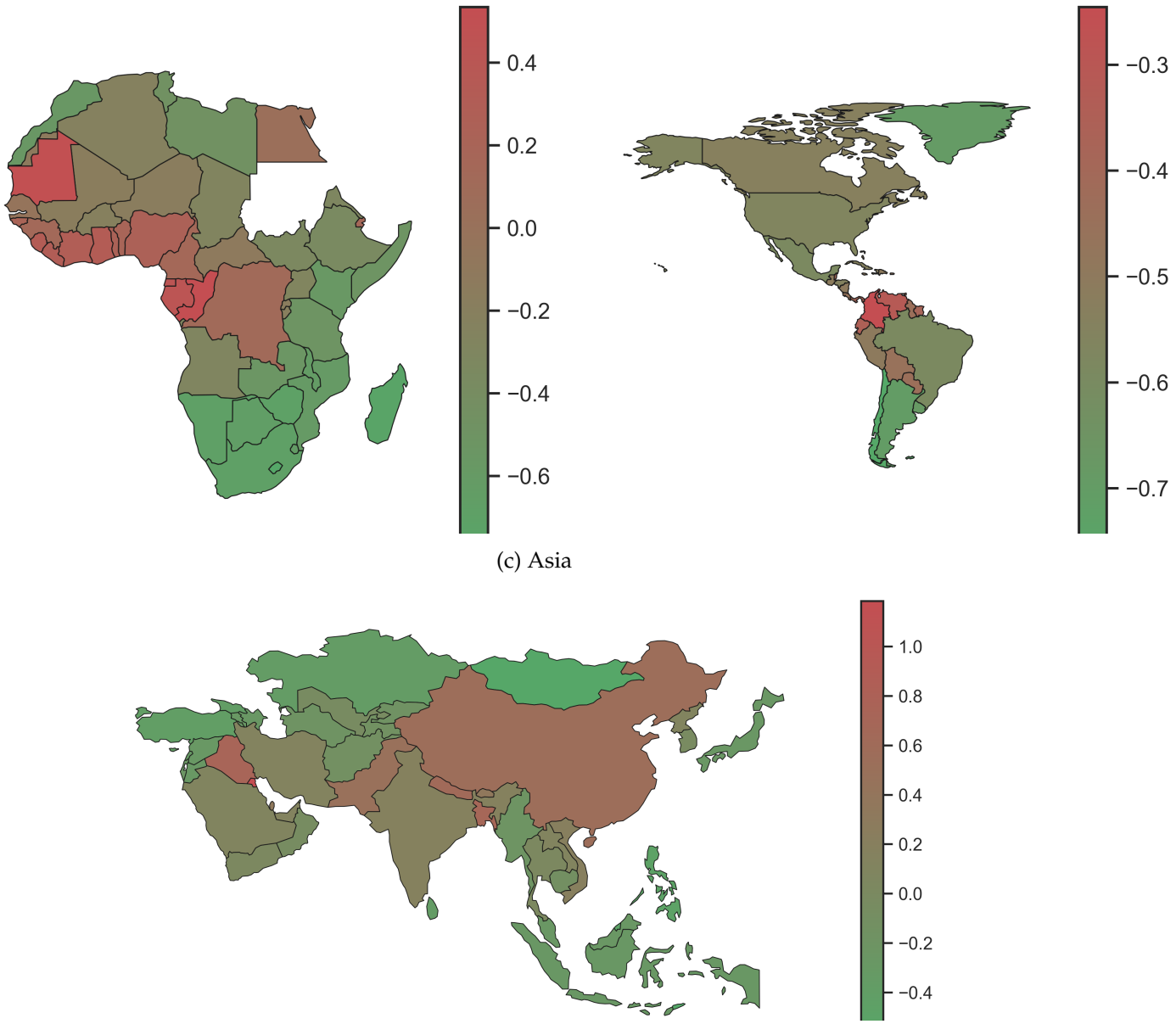

Note: The panels present the continent-specific relative dispersion of air pollution by aerosols as measured by Aerosol Optical Depth (AOD). We compute annual average AOD for each cell ($1° \times 1°$ longitude–latitude grid) and then generate country-specific AOD as cell-population weighted averages. The colors in each Panel correspond to levels of what we call continental excess aerosol burden: A value of 0.5 (-0.5) indicates that a country's AOD measure is 50 percent greater (smaller) than the continental weighted mean. In all Panels, darker shades of green (red) correspond to greater magnitudes of negative (positive) excess burdens.

Figure E.10: Continental association between air pollution by aerosols and GDP per capita, 2010

(a) National scatter plots, national population weighted bivariate regression lines

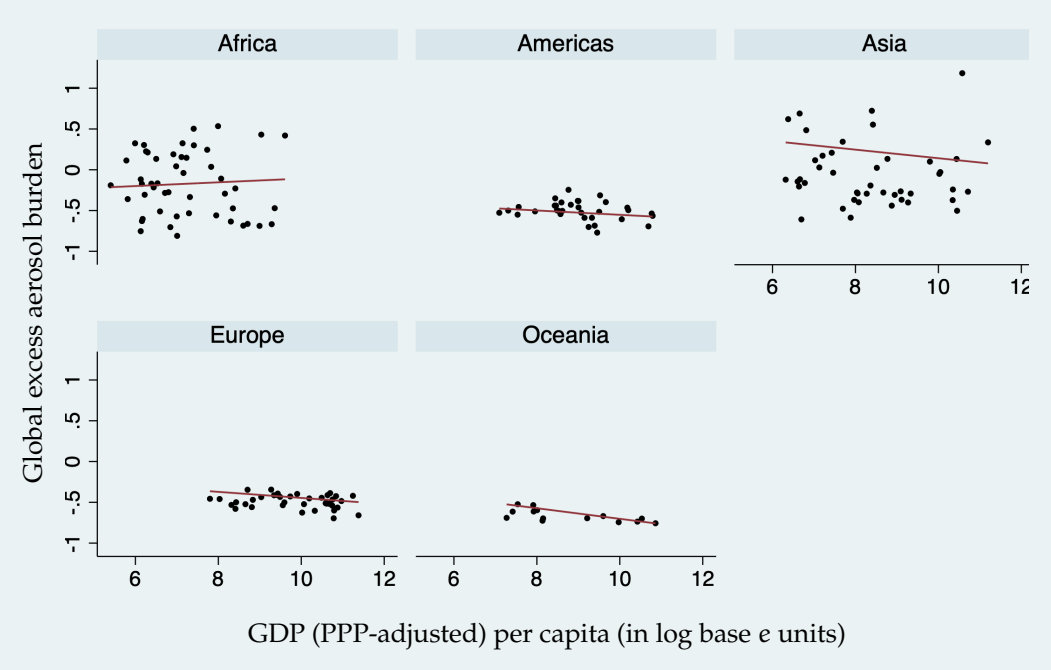

(b) Subnational scatter plots, subnational population weighted bivariate regression lines

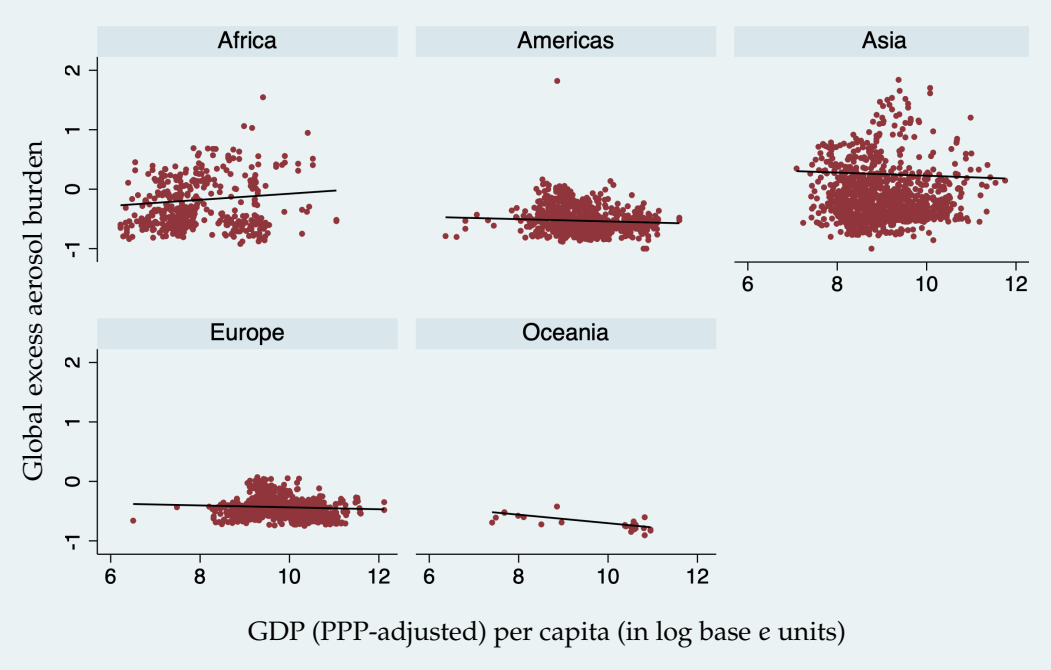

Notes: Across the panels, the x-axes correspond to levels of economic development as measured by GDP (Purchasing Price Parity adjusted) per capita in log base e units, and the y-axes correspond to relative exposures to air pollution by aerosols as measured by Aerosol Optical Depth (AOD). The y-axes across panels are in units of what we call global excess aerosol burden: A value of 0.5 (-0.5) indicates that a national or subnational unit's AOD measure is 50 percent greater (smaller) than the global weighted mean. We compute annual average AOD for each cell ($1^\circ \times 1^\circ$ longitude–latitude grid) and then generate national and subnational AOD as cell-population weighted averages. Subnational GDP and boundaries come from Kummu, Taka, and Guillaume (2018). See Figure 7 for global results and see Table 1 for regression coefficients.

Table E.1: Continental population-weighted distribution of air pollution by aerosols, 2010

	Population weighted means		Within-group AOD distributions	
Continent	AOD	Excess aerosol burden	P80 to P20 ratio	P90 to P10 ratio
Africa	0.37	-0.18	2.78	4.01
Americas	0.21	-0.54	1.56	2.23
Asia	0.57	0.25	2.25	3.18
Europe	0.25	-0.44	1.36	1.68
Oceania	0.14	-0.70	1.76	2.24

Note: The panels present key statistics from the global distribution of air pollution by aerosols as measured by Aerosol Optical Depth (AOD). In data columns 1 and 2, we show continent-specific population-weighted means. In data columns 3 and 4, we summarise within-continent AOD distributions using relative percentile ratios. The statistics in this table are computed based on the distribution of AOD and population across cells ($1^\circ \times 1^\circ$ longitude–latitude grid) corresponding to each continent. More specifically, the interpretation of AOD is that < 0.1 indicates crystal clear sky and AOD of 1 indicates very hazy conditions. For excess aerosol burden, a value of 0.5 (-0.5) indicates that a continent's AOD measure is 50 percent greater (smaller) than the global weighted mean. Finally, the P80 (P90) to P20 (P10) ratios are based on dividing the 80th (90th) percentile of the within continent AOD distribution by the 20th (10th) percentile of that distribution.

Table E.2: Global AOD in 2010

Location name	Excess burden	Excess burden rank	Mean AOD exposure	p20 AOD exposure	P80 AOD exposure	p80/p20 ratio	p90/p10 ratio
Panel A: Regions							
Asia	0.250	1	570.344	348.518	785.792	2.255	3.175
Africa	-0.180	2	374.305	193.571	538.424	2.782	4.013
Europe	-0.441	3	254.960	212.177	287.689	1.356	1.681
Americas	-0.544	4	207.836	156.255	243.476	1.558	2.232
Oceania	-0.701	5	136.313	103.840	182.795	1.760	2.241
Panel B: Sub regions							
Eastern Asia	0.464	1	668.134	369.572	957.117	2.590	3.240
Southern Asia	0.259	2	574.525	395.941	772.077	1.950	2.269
Western Africa	0.138	3	519.223	378.083	666.123	1.762	2.265
Middle Africa	0.016	4	463.605	305.944	617.175	2.017	2.540
Western Asia	-0.144	5	390.507	260.853	509.528	1.953	2.726
South-eastern Asia	-0.188	6	370.400	249.775	462.960	1.854	2.457
Northern Africa	-0.196	7	366.934	196.316	457.041	2.328	2.936
Central Asia	-0.199	8	365.381	266.444	437.113	1.641	2.103
Eastern Europe	-0.385	9	280.816	235.193	302.142	1.285	1.737
Western Europe	-0.446	10	252.816	219.301	280.139	1.277	1.514
Eastern Africa	-0.470	11	241.793	162.009	315.269	1.946	2.636
Caribbean	-0.506	12	225.326	199.155	246.721	1.239	1.308
Northern Europe	-0.519	13	219.472	180.145	245.138	1.361	1.581
South America	-0.523	14	217.508	145.292	308.824	2.126	3.174
Southern Europe	-0.526	15	216.390	171.630	249.351	1.453	1.798
Melanesia	-0.549	16	205.557	182.795	224.981	1.231	1.674
Northern America	-0.562	17	200.015	168.642	226.820	1.345	1.668
Central America	-0.566	18	198.101	167.071	228.240	1.366	1.789
Micronesia	-0.659	19	155.536	141.417	155.216	1.098	1.333
Southern Africa	-0.688	20	142.460	101.679	175.641	1.727	2.105
Polynesia	-0.728	21	123.999	122.737	125.451	1.022	1.065
Australia and New Zealand	-0.753	22	112.690	97.169	125.867	1.295	1.577
Panel C: Countries							
Kuwait	1.184	1	996.200	996.200	996.200	1.000	1.000
Iraq	0.723	2	786.001	669.404	746.549	1.115	1.321
Bangladesh	0.690	3	770.832	771.527	785.792	1.018	1.122
Nepal	0.620	4	739.015	686.867	799.155	1.163	1.450
China	0.553	5	708.502	456.094	964.901	2.116	3.163
Congo	0.535	6	699.939	657.733	757.810	1.152	1.229
Mauritania	0.503	7	685.611	226.053	515.221	2.279	18.191

Continued on next page

Table E.2: Global AOD in 2010

Location name	Excess burden	Excess burden rank	Mean AOD exposure	p20 AOD exposure	P80 AOD exposure	p80/p20 ratio	p90/p10 ratio
Pakistan	0.485	8	677.484	442.175	841.764	1.904	2.322
Gabon	0.431	9	652.738	617.487	688.877	1.116	1.158
Equatorial Guinea	0.420	10	647.543	647.543	647.543	1.000	1.000
Bhutan	0.344	11	613.163	586.935	622.777	1.061	1.061
Qatar	0.336	12	609.186	600.623	636.072	1.059	1.059
Ghana	0.325	13	604.349	580.436	649.359	1.119	1.295
Sierra Leone	0.324	14	604.054	598.463	608.526	1.017	1.017
Liberia	0.304	15	594.627	597.001	597.001	1.000	1.016
Côte d'Ivoire	0.300	16	592.938	557.696	619.125	1.110	1.178
Nigeria	0.245	17	567.854	410.404	727.731	1.773	2.061
Togo	0.226	18	559.068	414.002	602.677	1.456	1.472
Guinea-Bissau	0.213	19	553.339	551.990	551.990	1.000	1.000
Viet Nam	0.208	20	551.183	403.817	798.375	1.977	2.620
Benin	0.190	21	542.579	486.579	601.623	1.236	1.294
India	0.172	22	534.773	385.498	743.722	1.929	2.196
Djibouti	0.156	23	527.295	480.416	554.850	1.155	1.155
Cameroon	0.147	24	523.082	312.068	689.956	2.211	2.439
Iran (Islamic Republic of)	0.134	25	517.044	357.649	594.551	1.662	2.560
Guinea	0.134	26	517.011	480.625	538.424	1.120	1.509
United Arab Emirates	0.133	27	516.597	486.496	537.271	1.104	1.326
Democratic People's Republic of Korea	0.119	28	510.395	369.168	601.629	1.630	1.845
Lao People's Democratic Republic	0.117	29	509.306	489.368	539.400	1.102	1.249
Democratic Republic of the Congo	0.113	30	507.867	426.386	630.865	1.480	1.875
Saudi Arabia	0.100	31	501.745	374.105	602.772	1.611	2.344
Sao Tome and Principe	0.042	32	475.475	475.664	475.664	1.000	1.000
Egypt	0.036	33	472.604	454.804	504.682	1.110	1.269
Yemen	0.028	34	469.093	426.086	513.570	1.205	1.425
Thailand	0.024	35	466.970	371.127	563.575	1.519	1.898
Republic of Korea	-0.029	36	442.932	374.747	476.859	1.272	1.391
Uzbekistan	-0.036	37	439.572	369.474	491.421	1.330	1.618
Senegal	-0.039	38	438.298	393.258	497.312	1.265	2.015
Oman	-0.050	39	433.497	352.272	485.810	1.379	1.747
Cabo Verde	-0.109	40	406.388	397.570	417.401	1.050	1.082
Cambodia	-0.116	41	403.174	372.865	462.888	1.241	1.241

Continued on next page

Table E.2: Global AOD in 2010

Location name	Excess burden	Excess burden rank	Mean AOD exposure	p20 AOD exposure	P80 AOD exposure	p80/p20 ratio	p90/p10 ratio
Central African Republic	-0.117	42	402.609	364.299	431.582	1.185	1.301
NA	-0.118	43	402.441	286.730	487.305	1.700	1.700
Afghanistan	-0.121	44	400.702	335.589	401.973	1.198	1.388
Western Sahara	-0.129	45	397.188	311.603	456.174	1.464	1.629
Tajikistan	-0.144	46	390.276	327.683	456.403	1.393	1.458
Kyrgyzstan	-0.162	47	382.302	287.899	487.359	1.693	1.883
Mali	-0.166	48	380.276	334.256	414.822	1.241	1.613
Rwanda	-0.171	49	378.144	368.029	400.966	1.089	1.089
Niger	-0.173	50	377.227	295.893	435.561	1.472	1.761
Burundi	-0.191	51	369.184	356.733	411.344	1.153	1.153
Turkmenistan	-0.193	52	367.939	309.959	429.385	1.385	1.465
Myanmar	-0.205	53	362.445	320.250	393.409	1.228	1.648
Burkina Faso	-0.216	54	357.620	303.564	407.795	1.343	1.388
Algeria	-0.229	55	351.581	147.950	204.541	1.382	1.596
Israel	-0.242	56	345.721	346.908	346.908	1.000	1.000
Colombia	-0.246	57	344.093	290.670	373.657	1.286	1.552
Malaysia	-0.264	58	335.477	264.712	389.021	1.470	1.641
Japan	-0.269	59	333.423	309.437	349.926	1.131	1.233
Chad	-0.275	60	330.462	262.418	407.539	1.553	2.112
Indonesia	-0.279	61	329.062	240.824	385.402	1.600	2.014
Azerbaijan	-0.279	62	328.985	304.473	372.522	1.223	1.656
Uganda	-0.284	63	326.744	245.289	395.805	1.614	1.789
Armenia	-0.289	64	324.067	296.450	352.946	1.191	1.191
Syrian Arab Republic	-0.292	65	323.019	269.709	348.202	1.291	1.536
Angola	-0.293	66	322.536	205.641	477.754	2.323	2.609
Jordan	-0.293	67	322.356	120.000	421.559	3.513	3.513
Eritrea	-0.306	68	316.446	274.813	301.446	1.097	1.259
Lebanon	-0.308	69	315.848	315.848	315.848	1.000	1.000
Venezuela (Bolivarian Republic of)	-0.313	70	313.181	260.293	375.983	1.444	1.845
South Sudan	-0.334	71	303.670	277.305	338.961	1.222	1.459
Russian Federation	-0.344	72	299.203	226.002	379.103	1.677	2.303
Belarus	-0.346	73	298.358	281.522	317.995	1.130	1.174
Ecuador	-0.350	74	296.317	249.103	337.712	1.356	1.366
Ethiopia	-0.360	75	292.012	264.896	328.376	1.240	1.588
Bonaire, Sint Eustatius and Saba	-0.360	76	291.891	291.891	291.891	1.000	1.000
Kazakhstan	-0.368	77	288.351	224.732	329.436	1.466	1.629
Sri Lanka	-0.369	78	287.907	277.762	304.883	1.098	1.120

Continued on next page

Table E.2: Global AOD in 2010

Location name	Excess burden	Excess burden rank	Mean AOD exposure	p20 AOD exposure	P80 AOD exposure	p80/p20 ratio	p90/p10 ratio
Cyprus	-0.373	79	286.200	269.698	294.974	1.094	1.094
Suriname	-0.381	80	282.335	237.388	323.379	1.362	1.374
Panama	-0.383	81	281.627	243.148	330.766	1.360	1.405
Belgium	-0.387	82	279.568	281.810	301.771	1.071	1.488
Poland	-0.393	83	276.894	259.834	290.006	1.116	1.168
Trinidad and Tobago	-0.397	84	275.181	260.036	308.829	1.188	1.291
Czechia	-0.397	85	274.978	272.064	277.918	1.022	1.095
Georgia	-0.398	86	274.533	214.548	308.815	1.439	1.512
Belize	-0.401	87	273.265	269.179	290.550	1.079	1.153
Türkiye	-0.401	88	272.982	244.503	301.157	1.232	1.417
Lithuania	-0.409	89	269.621	267.599	280.714	1.049	1.252
Germany	-0.412	90	268.417	246.370	291.907	1.185	1.292
Latvia	-0.413	91	267.779	249.366	286.085	1.147	1.214
Switzerland	-0.420	92	264.545	216.212	335.231	1.550	1.550
Netherlands (Kingdom of the)	-0.424	93	262.608	229.095	276.623	1.207	1.468
Slovakia	-0.428	94	260.832	258.843	263.547	1.018	1.031
Grenada	-0.429	95	260.454	260.454	260.454	1.000	1.000
Hungary	-0.434	96	258.215	240.479	273.564	1.138	1.177
Romania	-0.436	97	257.135	240.783	274.301	1.139	1.194
Guyana	-0.440	98	255.597	235.630	260.848	1.107	1.205
Maldives	-0.440	99	255.539	223.449	304.718	1.364	1.364
Paraguay	-0.440	100	255.270	241.772	256.170	1.060	1.337
Italy	-0.444	101	253.369	211.530	338.032	1.598	1.681
Greece	-0.452	102	250.091	239.239	263.787	1.103	1.127
French Guiana	-0.455	103	248.724	238.593	258.310	1.083	1.083
Bolivia (Plurinational State of)	-0.456	104	248.142	107.765	469.105	4.353	5.356
Republic of Moldova	-0.457	105	247.883	247.711	248.001	1.001	1.001
Ukraine	-0.459	106	246.656	222.327	266.884	1.200	1.304
Costa Rica	-0.461	107	245.835	246.355	246.355	1.000	1.000
Puerto Rico	-0.465	108	244.158	244.946	244.946	1.000	1.000
Austria	-0.465	109	244.017	222.423	299.735	1.348	1.351
Bulgaria	-0.469	110	242.064	217.991	262.141	1.203	1.263
Libya	-0.471	111	241.281	85.000	390.648	4.596	7.031
Tunisia	-0.474	112	240.124	195.124	259.774	1.331	1.562
Philippines	-0.477	113	238.324	214.698	265.676	1.237	1.324
Denmark	-0.484	114	235.295	220.436	263.800	1.197	1.279
Anguilla	-0.486	115	234.217	234.551	234.551	1.000	1.000
Bahamas	-0.495	116	230.266	183.303	255.483	1.394	1.394

Continued on next page

Table E.2: Global AOD in 2010

Location name	Excess burden	Excess burden rank	Mean AOD exposure	p20 AOD exposure	P80 AOD exposure	p80/p20 ratio	p90/p10 ratio
Jamaica	-0.497	117	229.271	229.271	229.271	1.000	1.000
North Macedonia	-0.499	118	228.442	217.074	240.600	1.108	1.108
Nicaragua	-0.500	119	228.106	200.614	267.512	1.333	1.333
Estonia	-0.501	120	227.512	221.252	243.488	1.101	1.237
Brunei Darussalam	-0.503	121	226.775	226.775	226.775	1.000	1.000
Dominican Republic	-0.505	122	225.985	205.171	246.721	1.203	1.203
Peru	-0.505	123	225.921	150.360	306.724	2.040	2.513
Somalia	-0.509	124	223.871	140.671	304.921	2.168	2.913
Guatemala	-0.511	125	223.228	215.362	259.368	1.204	1.564
United Republic of Tanzania	-0.511	126	223.098	159.251	296.760	1.863	2.732
United Kingdom of Great Britain and Northern Ireland	-0.511	127	223.082	190.958	245.138	1.284	1.534
France	-0.515	128	221.071	186.523	263.557	1.413	1.551
Antigua and Barbuda	-0.516	129	220.818	220.818	220.818	1.000	1.000
Iceland	-0.518	130	219.993	174.424	244.077	1.399	1.497
British Virgin Islands	-0.522	131	218.175	218.175	218.175	1.000	1.000
Slovenia	-0.522	132	217.887	220.413	220.413	1.000	1.092
Serbia	-0.523	133	217.725	196.285	239.833	1.222	1.282
Papua New Guinea	-0.524	134	217.328	195.152	229.221	1.175	1.324
Saint Lucia	-0.526	135	216.015	216.015	216.015	1.000	1.000
Haiti	-0.527	136	215.682	218.867	222.296	1.016	1.171
Martinique	-0.528	137	215.211	215.211	215.211	1.000	1.000
Albania	-0.532	138	213.665	193.875	237.533	1.225	1.260
Zambia	-0.533	139	212.904	194.906	228.371	1.172	1.416
Vanuatu	-0.534	140	212.481	212.332	217.411	1.024	1.024
Croatia	-0.535	141	211.872	194.553	224.213	1.152	1.243
Canada	-0.536	142	211.674	194.535	232.380	1.195	1.356
Montserrat	-0.537	143	210.979	210.979	210.979	1.000	1.000
Finland	-0.540	144	209.848	196.782	221.343	1.125	1.272
Cuba	-0.544	145	208.080	195.543	222.049	1.136	1.257
Honduras	-0.551	146	204.951	181.175	228.240	1.260	1.342
Montenegro	-0.559	147	201.253	201.253	201.253	1.000	1.000
Morocco	-0.559	148	201.068	176.979	214.546	1.212	1.382
Sweden	-0.564	149	198.651	176.150	219.335	1.245	1.405
United States of America	-0.565	150	198.414	165.615	226.184	1.366	1.715
Kenya	-0.572	151	195.193	162.009	210.215	1.298	1.700

Continued on next page

Table E.2: Global AOD in 2010

Location name	Excess burden	Excess burden rank	Mean AOD exposure	p20 AOD exposure	P80 AOD exposure	p80/p20 ratio	p90/p10 ratio
Bosnia and Herzegovina	-0.580	152	191.643	185.445	197.183	1.063	1.063
Mongolia	-0.587	153	188.282	113.609	258.383	2.274	2.707
Brazil	-0.589	154	187.608	147.164	200.481	1.362	2.211
Mexico	-0.589	155	187.512	159.380	204.006	1.280	1.732
Marshall Islands	-0.595	156	184.592	181.503	186.102	1.025	1.047
Ireland	-0.600	157	182.617	160.583	190.159	1.184	1.434
Mozambique	-0.603	158	181.125	139.031	231.532	1.665	2.023
Spain	-0.604	159	180.803	157.026	203.778	1.298	1.658
Turks and Caicos Islands	-0.607	160	179.385	179.194	179.194	1.000	1.000
Timor-Leste	-0.609	161	178.543	171.897	193.745	1.127	1.170
Micronesia (Federated States of)	-0.612	162	176.857	170.966	183.043	1.071	1.200
Solomon Islands	-0.614	163	176.231	170.552	178.997	1.050	1.151
Portugal	-0.626	164	170.721	167.203	183.161	1.095	1.145
Malawi	-0.629	165	169.087	149.646	179.473	1.199	1.313
Eswatini	-0.635	166	166.508	166.508	166.508	1.000	1.000
Norway	-0.659	167	155.594	139.781	169.569	1.213	1.314
Botswana	-0.664	168	153.210	114.018	174.323	1.529	2.086
Seychelles	-0.667	169	151.727	151.217	151.217	1.000	1.000
Northern Mariana Islands	-0.669	170	151.054	137.324	155.216	1.130	1.130
Uruguay	-0.685	171	143.515	124.340	152.836	1.229	1.470
Namibia	-0.685	172	143.512	89.554	232.306	2.594	2.919
South Africa	-0.688	173	142.232	102.360	175.641	1.716	2.105
Kiribati	-0.690	174	141.200	141.417	141.417	1.000	1.000
Greenland	-0.694	175	139.666	127.995	164.399	1.284	1.713
Palau	-0.695	176	139.039	137.363	142.242	1.036	1.036
Faroe Islands	-0.696	177	138.608	138.608	138.608	1.000	1.000
Fiji	-0.697	178	138.105	125.701	145.010	1.154	1.224
New Caledonia	-0.700	179	137.022	134.252	134.252	1.000	1.128
Argentina	-0.701	180	136.339	97.144	163.626	1.684	2.135
Zimbabwe	-0.704	181	135.119	117.070	149.602	1.278	1.606
Wallis and Futuna Islands	-0.724	182	125.714	125.591	125.591	1.000	1.000
Tonga	-0.725	183	125.336	125.451	125.451	1.000	1.000
Cook Islands	-0.731	184	122.776	122.737	122.737	1.000	1.000
New Zealand	-0.737	185	120.175	103.840	134.543	1.296	1.437
French Polynesia	-0.744	186	116.952	114.651	120.304	1.049	1.117

Continued on next page

Table E.2: Global AOD in 2010

Location name	Excess burden	Excess burden rank	Mean AOD exposure	p20 AOD exposure	P80 AOD exposure	p80/p20 ratio	p90/p10 ratio
Madagascar	-0.753	187	112.744	74.526	160.918	2.159	3.361
Falkland Islands (Malvinas)	-0.755	188	111.690	108.658	116.828	1.075	1.148
Australia	-0.756	189	111.140	97.169	125.867	1.295	1.489
Chile	-0.770	190	104.689	82.714	111.505	1.348	1.572
Lesotho	-0.810	191	86.471	90.216	90.216	1.000	1.408

Note: A rank of 1 indicates that the location has the highest excess burden among the other locations in the geographic category. Locations are divided into three geographic units, regions, sub regions, and countries. Results are based on within-country distributions of cell-level population distribution as well as cell-level air pollution by aerosol distributions. Atmospheric pollution by aerosols is important to human health and well-being because higher amounts of aerosol particles degrade visibility and can also damage health, especially when there is a higher concentration of $PM_{2.5}$ particles that are smaller than 2.5 micrometers. Aerosol Optical Depth (AOD) is a satellite-based measure that captures the composition, sizes, and concentration of aerosols by measuring the magnitudes of atmospheric light reflection and absorption across the globe. AOD < 0.1 indicates crystal clear sky and AOD of 1 indicates very hazy conditions.